Higher-Moment Risk[*]

Niels Joachim Gormsen[†]and Christian Skov Jensen[‡]

December 2023

Abstract

We study time variation in the shape of the distribution of stock returns. In a global sample covering 17 countries, returns are more left skewed and fat tailed during good times than during bad times. This pattern creates pro-cyclical variation in conditional tail risk, which is the risk of losing several conditional standard deviations of returns. The variation in higher-order moments is hard to reconcile with the idea that disaster risk is elevated in bad times, which is otherwise a basic premise of leading disaster-based asset pricing models.

1   Introduction

The shape of the distribution of stock returns plays a key role in asset pricing. A large literature documents how deviations of the return distribution from the normal distribution induces tail risk and that exposure to such tail risk is being compensated in asset markets (see e.g. Kelly and Jiang, 2014; Giglio, Kelly, and Pruitt, 2016; Bali and Murray, 2013; Bali, An, Ang, and Cakici, 2014; Jiang, Wu, Zhou, and Zhu, 2020). Another line of research on disaster-based asset pricing argues that the deviation from the normal distribution helps justify the high and time varying equity risk premium (Barro, 2006; Gabaix, 2012; Wachter, 2013).

We document strong cyclical variation in the shape of the return distribution. In a broad global sample, we consistently find that the shape of the return distribution is more left skewed and fat tailed during good times than during bad times. We illustrate this variation in Figure 1, in which we define good and bad times based on the ex ante volatility of stock return. The figure plots the risk-neutral return distribution for S&P 500 for a day with low volatility and for a day with high volatility. The distribution is notably more left skewed and fat tailed on the low volatility day (good times) than on the high volatility day (bad times). The shape of the distribution of stock returns is thus riskier during good times than during bad times, in the sense that there is relatively more mass in the left tail of the distribution. This pattern generalizes across our sample and across different measures of good and bad times.

We document our results in a broad global sample covering stock market indexes in 17 countries. Through most of the paper, we study and summarize the shape of the return distribution by the behavior of its higher-order moments. We focus particularly on the third and fourth standardized moments, which capture the skewness and kurtosis of a distribution.[1] We study the behavior of both ex post realized moments and ex ante expected moments as estimated in a broad global sample of option prices. Our sample of option prices runs from 1996 and contains 20 different stock markets spread across the US, Europe, and Asia.

We first document a strong comovement between skewness and kurtosis. The two moments are strongly negatively correlated, which suggests there are periods where the return distribution is both more left skewed and more fat tailed. Both of these characteristics makes the shape of the return distribution riskier in the eyes of most risk averse investors, in the sense that they would lead to a lower expected utility than a normal distribution with the

---

[1]We consider standardized, as opposed to raw, moments throughout, as raw moments reflects both the shape of the return distribution and the level of variance.
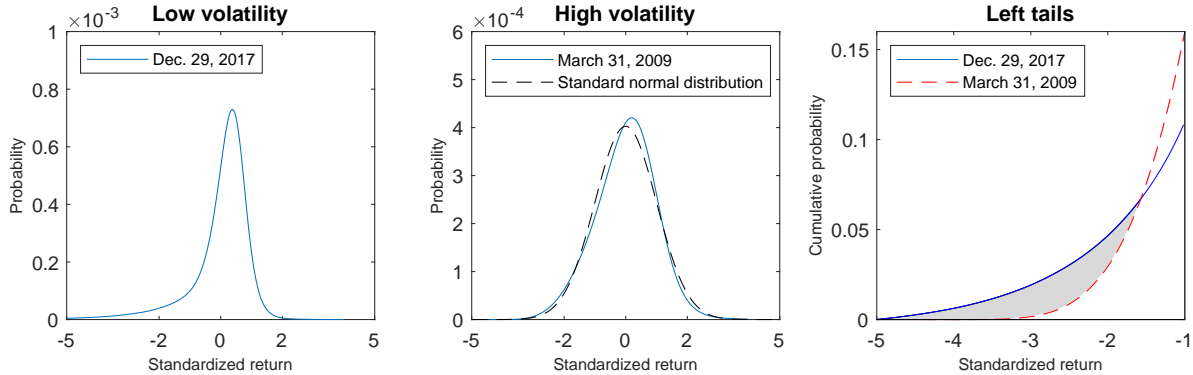
Figure 1: **Standardized risk-neutral distributions.** The figure shows the (standardized) risk neutral distribution for the S&P 500 on December 29, 2017 (left) and on March 31, 2009 (middle). Standardized return$_t$ = (return$_t$ − mean$_t$)/standard deviation$_t$. The standardized distributions are re-scaled to integrate to one. The distributions are for quarterly horizon returns.

same mean and variance would.[2] On the other hand, there are periods where the shape of the return distribution is relatively safe, in the sense that it is close to a normal distribution and thus does not contain any "excess" probability of tail losses. The result holds both for realized and expected moments, and it is statistically significant on the quarterly horizon in each of the 20 stock markets we study.

More importantly, there are strong cyclical fluctuations in the higher-order moments of the return distribution. During good times, the distribution is more left skewed (skewness is more negative) and fat tailed (kurtosis more positive) than during bad times. The shape of the distribution is thus riskier during good times than bad times. This result holds across expected and realized moments and across many different definitions of good and bad times, including definitions based on volatility, valuation ratios, recessions, and measures of real economic activity. Higher-order moments thus tend to make the distribution of returns riskier during good times than bad times. This cyclical variation in higher-moment risk is opposite that of the second moments, which makes the distribution riskier during bad times (i.e., variance increases during bad times).

The variation in higher-order moments influence the tail risk in the distribution of market returns. It is useful to separate between two different types of tail risk. One measure of tail risk is the probability of an *unconditional* tail loss. This could, for instance, be the probability of observing an unexpected loss of 30% or more over the subsequent month. This probability is influenced by the variance of the distribution as well as the skewness, kurtosis, and other

---

[2]For some investors, such as investors with quadratic utility, the expected utility is not influenced by the variation in higher-order moments.

higher-order moments. The literature has carefully studied this type of tail risk, finding that it generally peaks in bad times (Kelly and Jiang, 2014; Bollerslev and Todorov, 2011b). It would be natural to conjecture that this increase in tail risk is, at least in part, driven by the distribution becoming more left skewed and fat tailed, but this is not the case. We show that the increase in unconditional tail risk during bad times is driven by an increase in the standard deviation, not by the higher-order moments of the distribution. Higher-order moments, in fact, serve to reduce the total amount of tail risk during bad times.

In contrast to the above literature, we focus on *conditional* tail risk, which is the probability of observing a loss of X conditional standard deviations. This tail probability is driven by the higher-order moments, and is informative about the riskiness of the shape of the distribution. This tail probability has broad implications for investors and regulators, as discussed shortly.

We document that the conditional tail risk is pro-cyclical, as expected given the variation in higher-order moments. We estimate tail loss probabilities from option prices using both a non-parametric method based on Breeden and Litzenberger (1978) as well as a parametric approach from Bollerslev, Todorov, and Xu (2015). Both methods produce conditional tail probabilities that are larger when skewness is more negative and kurtosis is more positive. The tail probabilities are pro-cyclical as they increase during good times and decrease during bad times, hitting the lowest values during the global financial crisis. During bad times, the conditional tail loss probabilities come close to those predicted by a normal distribution, which is to say that there is very little risk coming from higher-order moments during these periods.

The fact that higher-moment risk disappears in bad times is hard to reconcile with the idea that these are periods with high disaster risk, as argued by a large literature in asset pricing (Tsai and Wachter 2015). Disaster risk is often thought of as an elevated probability of observing very negative returns (driven by large, negative jumps). The possibility of such disastrous returns should, everything else equal, make the return distribution more left skewed and fat tailed. However, the return distribution is close to the normal distribution during bad times, which means that very positive returns are as likely as very negative returns during these periods. We show, through studies of leading disaster models by Gabaix (2012) and Wachter (2013), that such variation in the shape of the distribution is difficult to reconcile with the notion that bad times are periods of elevated disaster risk. In these models, elevated disaster risk indeed results in a more left skewed and fat tailed distribution of returns. The results thus question whether bad times are periods with elevated disaster risk – and by

extension, whether the high risk premia observed during bad times are compensation for elevated disaster risk.

Our findings on disaster risk are consistent with recent research by Baron, Xiong, and Ye (2023). The authors construct an objective measure of disaster risk across a global panel of 20 countries from 1870 to 2021. The authors find that disaster risk is not elevated during what is usually referred to as "bad times" in asset pricing, namely periods with low valuation ratios and high equity risk premia. Instead, disaster risk appears to be elevated a few years before bad times materialize, which is consistent with our finding that higher-moment risk peaks during good times, such as just before the global financial crisis.[3] The results are also consistent with Dew-Becker and Giglio (2023), who show that the largest observed crashes in the market portfolio are not driven by jumps. Instead, the authors argue that these crashes are predated by a substantial increase in diffusive volatility, and that the crashes are driven by the diffusive element in returns rather than jumps.

While the fluctuations in higher-order moments are fundamentally at odds with disaster models, they are straightforward to account for in reduced-form jump diffusion models. The fluctuations in skewness, for instance, can qualitatively be accounted for with a jump diffusion model with stochastic volatility and constant jump intensity in returns (with jumps being negative on average). In such a model, the skewness is generally a product of two opposing forces: the negative jumps push towards a more left skewed distribution while the diffusive volatility push towards a more symmetric distribution. When diffusive volatility is elevated, the diffusive volatility plays a relatively larger role and the distribution thus becomes more symmetric. On the other hand, when diffusive volatility is very low, the jump component plays a relatively larger role and the distribution thus becomes more left skewed. Eraker, Johannes, and Polson (2003) estimate a series of jump diffusion models to stock returns and find that a model with stochastic volatility and constant jumps provides the best fit. The variation in skewness that we uncover is thus consistent with findings of the previous literature based on jump diffusion models (see Section 4 for further discussion).

The cyclical fluctuations in higher-moment risk has direct implications for investors and regulators. Regulators are often interested in measuring and controlling the probability of tail events. For instance, the Basel regulation requires banks and other financial institutions to report and control the value-at-risk for their assets. Our results suggest that measures only based on variance are likely to understate the true risk of portfolios that contain equities.

---

[3]Muir (2017) further questions the extent to which financial fluctuations are driven by macroeconomic risks.

More importantly, this mistake is going to be the largest during good times with low variance and high prices, which are potentially periods where regulators should worry about over-accumulation of risk in the economy. Moreover, many investors follow volatility-managed strategies (Moreira and Muir 2017) in the hope of keeping portfolio risk constant over time. However, the cyclical fluctuations in higher-moment risk translates directly into cyclical fluctuations in riskiness of such portfolios, which we show can be substantial.

The paper proceeds as follows. Section 2 explains our main methodology and data. Section 3 documents time variation in higher-order moments. Section 4 estimates conditional tail risk. Section 5 relates our findings to disaster-based asset pricing models. Section 6 concludes.

2   Methodology

We summarize the shape of the return distribution through the behavior of the standardized moments. As is well known, the third standardized moment captures the skewness of a distribution while the fourth standardized moment captures the mass in the tails of a distribution. We estimate the conditional moments of stock market returns in two ways: (i) we infer the ex ante moments of stock market returns using the forward-looking information in current and observable asset prices and (ii) we estimate the ex post realized moments of stock market returns using the backward-looking information in past realized returns. Section 2.1 explains how we estimate ex ante moments from option prices and Section 2.2 explains how we estimate ex post realized moments. In Section 2.3, we discuss summary statistics of the inferred moments and run predictive regressions of realized moments onto expected moments.

2.1   Inferring Ex Ante Stock Market Moments from Asset Prices

Breeden and Litzenberger (1978), Bakshi and Madan (2000), and Bakshi, Kapadia, and Madan (2003) shows that the arbitrage free price of a claim to a future (twice differentiable) payoff can be expressed in terms of a continuum of put and call option prices. Specifically, we can write the n'th risk-neutral raw moment of stock market returns, $R_{t,T}$, as:

$$E_t[R_{t,T}^n] = (R_{t,T}^f)^n + R_{t,T}^f \left[p(n) + c(n) \right], \tag{1}$$

with

$$p(n) = \int_0^{F_{t,T}} \frac{n(n-1)}{S_t^n} \left(S_t R_{t,T}^f - F_{t,T} + K \right)^{n-2} \mathrm{put}_{t,T}(K) dK \tag{2}$$

$$c(n) = \int_{F_{t,T}}^{\infty} \frac{n(n-1)}{S_t^n} \left(S_t R_{t,T}^f - F_{t,T} + K \right)^{n-2} \mathrm{call}_{t,T}(K) dK, \tag{3}$$

where $F_{t,T}$ is the forward price, $R_{t,T}^f$ is the gross risk-free rate, and $\mathrm{call}_{t,T}(K)$ and $\mathrm{put}_{t,T}(K)$ are call and put option prices written on the stock market at time t with horizon $T-t$ and strike K.

Since we do not observe a continuum of call and put option prices, we numerically approximate the integrals in Equation (2) in the data. We write the price at time t of an out-of-the money option with strike K and maturity T as

$$\Omega_{t,T}(K) = \begin{cases} \mathrm{call}_{t,T}(K) & \text{if } K \geq F_{t,T} \\ \mathrm{put}_{t,T}(K) & \text{if } K < F_{t,T}. \end{cases} \tag{4}$$

We let $K_1, ..., K_N$ be the (increasing) sequence of observable strikes for the N out-of-the money put and call options and define $\Delta K_i = \frac{K_{i+1} - K_{i-1}}{2}$ with

$$\Delta K_i = \begin{cases} K_{i+1} - K_i & \text{if } i = 1 \\ K_i - K_{i-1} & \text{if } i = N. \end{cases} \tag{5}$$

With this notation, we approximate the integrals in Equation (2) by observable sums such that the n'th risk-neutral raw moment becomes:

$$E_t[R_{t,T}^n] = (R_{t,T}^f)^n + R_{t,T}^f \left[\sum_{i=1}^{N} \frac{n(n-1)}{S_t^n} (S_t R_{t,T}^f - F_{t,T} + K_i)^{n-2} \Omega_{t,T}(K_i) \Delta K_i \right] \tag{6}$$

We obtain the standardized moments by combining Equation (6) for different values of n and using the standardized moment formula. Specifically, the ex ante risk-neutral skewness is:

$$\mathrm{Skewness}_{t,T} = \frac{E_t[R_{t,T}^3] - 3E_t[R_{t,T}](E_t[R_{t,T}^2] - E_t[R_{t,T}]^2) - E_t[R_{t,T}]^3}{(E_t[R_{t,T}^2] - E_t[R_{t,T}]^2)^{3/2}} \tag{7}$$

and the ex ante risk-neutral kurtosis is:

$$\text{Kurtosis}_{t,T} = \frac{E_t[R_{t,T}^4] - 3E_t[R_{t,T}]^4 + 6E_t[R_{t,T}]^2 E_t[R_{t,T}^2] - 4E_t[R_{t,T}]E_t[R_{t,T}^3]}{(E_t[R_{t,T}^2] - E_t[R_{t,T}]^2)^2} \quad (8)$$

We use data from the Ivy DB databases from OptionMetrics to extract information on vanilla call and put options written on the stock market indexes. We consider a total of twenty stock market indexes around the world. The data on US indexes spans the period from January 1996 to December 2020, the European data spans the period from January 2002 to January 2021, and the Asian data is from August 2004 to December 2019.

We do not observe options on all maturities. We therefore interpolate (or extrapolate if needed) standardized moments across maturities. As a robustness check, we also consider the alternative of estimating moments using the interpolated option prices in the volatility surface files from the Ivy DB US database in OptionMetrics. This database contains information on options written on US indexes that have standardized maturities and strikes (in the form of option deltas). Table A3 reports the pairwise correlations between the implied moments using either the standardized option data or the raw data. The correlations are lower for higher-order moments than for variances because the standardized data set contains fewer observations in the tails of the distributions and the higher-order moments are likely underestimated using this database. Nevertheless, we find that our main results, which we present in the next section, still hold when using the standardized option database.[4]

We also do not observe options for all strike prices. Throughout the paper, we use all observable prices. However, the number of available strikes increases over time, which might cause our moments to trend through time.[5] We consider several approaches to address this issue as explained in Appendix A. Overall, our results are robust to alternative choices related to the use of the observable option prices.

---

[4]See Table A4 for the US results using the standardized option database.

[5]As an example of this increase in traded option strikes throughout our sample, consider the S&P 500 index. In the beginning of our sample (Jan 1996), we observe option prices with strikes ranging from the spot price plus/minus three risk-neutral standard deviations. At the end of our sample (Dec 2020), we observe option prices with strikes as far as sixteen risk-neutral standard deviations into the tails of the distribution. This increase in options traded at different strikes might lead the estimated moments to be trending over time when we use all observable option prices simply because we have more information at the end of our sample than in the beginning. This fact is related to concerns put forth by Andersen and Bondarenko (2007) who note that option implied volatilities can be hard to measure accurately because of sparse coverage of option prices with strikes in the tails of the distribution.

2.2 Inferring Ex Post Realized Stock Market Moments

We compute conditional realized moments at the monthly and quarterly horizon. For variance, we apply the common method and use the sum of squared daily returns over the period as a measure of realized variance:

$$\text{Realized variance}_{t,T} = \sum_{s=t}^{T-1} r_{s,s+1}^2 \tag{9}$$

where $r_{s,s+1} = \log(R_{s,s+1})$ is the log-returns of the stock market between dates s and $s + 1$. We follow the methods of Neuberger (2012) and Bae and Lee (2021) to estimate realized skewness and kurtosis on monthly and quarterly horizon using daily data. In particular, we compute conditional realized skewness as

$$\text{Realized skewness}_{t,T} = \frac{\sum_{s=t}^{T-1} r_{s,s+1}^3 + 3 \times r_{s,s+1} \Delta M_{2,s+1,T}}{\text{Realized variance}_{t,T}^{3/2}}, \tag{10}$$

where $\Delta M_{2,s+1,T} = (M_{2,s+1,T} - M_{2,s,T})$ and $M_{2,s,T} = E_s[r_{s,T}^2]$ is the expected variance of log returns from time s to T,[6] and realized kurtosis as

$$\text{Realized kurtosis}_{t,T} = \frac{\sum_{s=t}^{T-1} r_{s,s+1}^4 + 6 \times r_{s,s+1}^2 \Delta M_{2,s+1,T} + 4 \times r_{s,s+1} \Delta M_{3,s+1,T} + 3 \times (\Delta M_{2,s+1,T})^2}{\text{Realized variance}_{t,T}^2} \tag{11}$$

where $\Delta M_{3,s+1,T} = (M_{3,s+1,T} - M_{3,s,T})$ and $M_{3,s,T} = E_s[r_{s,T}^3]$ is the expected third raw moment between times s and T.

In estimating the realized skewness and kurtosis, we need the expected raw moments in $\Delta M_{2,s+1,T}$ and $\Delta M_{3,s+1,T}$. These quantities are not directly observable in the data and we therefore follow Bae and Lee (2021) and compute these expectations under the risk-neutral measure using option prices as in Equation (6). We use moments for options with 30-day (90-day) maturity when inferring monthly (quarterly) horizon realized moments.[7]

---

[6]Neuberger (2012) uses a slightly different formulation of the third standardized moment than in Equation (10). We choose this formulation, which is used in Bae and Lee (2021), to describe skewness and kurtosis with similar mathematical formulation.

[7]In principle, the formula for the realized moments says that the horizon of the raw moments changes over the period. However, options are not available for all horizons on all days, which mean we cannot perfectly match the target horizons, leading us to the pragmatic solution of using 30-day (90-day for quarterly realized moments) options. We have experimented using expected raw moments with different horizons and we found that alternative choices have little impact on the realized moments. This conclusion aligns with results and

We note that these are proxies for the true realized moments as discussed in Bae and Lee (2021). In some cases, the estimates of realized kurtosis turns negative, which is a direct consequence of not observing the physical expected moments in $\Delta M_{2,s+1,T}$ and $\Delta M_{3,s+1,T}$ and not having data to perfectly match the horizons on these moments. Removing data points where the kurtosis is negative has little impact on the results.

2.3   Summary Statistics

Table 1 reports the average variance (annualized and in percentages), skewness, and kurtosis for the 20 stock markets in our sample. The table reports moments at the monthly and quarterly horizon for both the expected and realized moments. The table shows substantial dispersion in the average variance across stock markets. This is true for both implied and realized variance and at both the monthly and quarterly horizons. We find that both implied and realized skewness on average is negative for all indexes and at all horizons, suggesting that the stock market return distributions around the world feature the same directional tilting. Similarly, we find excess kurtosis (kurtosis> 3) for all stock markets in our sample, implying the return distributions on average have fatter tails than the normal distribution.

Before we head into our main empirical analysis, we ensure the ex ante implied moments predict the ex post realized moments. This serves both as a sanity check of the methodology and alleviates the concern that risk-neutral moments are poor proxies of realized moments. Previous work by Neuberger (2012), Bae and Lee (2021), and Dew-Becker (2021) already shows that ex ante option implied moments predict realized moments in the US, but we need to ensure that this result also holds in our broader international sample.

Figure 2 shows scatter plots of the average ex ante implied moments up against the respective average ex post realized moments. We find a strong positive and linear relationship between average ex ante variance and ex post realized variance. For monthly horizon variances, the slope coefficient is 0.73 and the adjusted R^2 is 53.7%. (A slope for variance that is less than one is expected due to the variance risk-premium, see e.g. Bollerslev, Tauchen, and Zhou (2009)). We find similar results for skewness and kurtosis, with R^2 ranging from 43% to 70% depending on the moment and the horizon. Overall, in averages, there is a strong linear relationship between the ex ante implied moments and the ex post realized moments.

To address the contemporaneous relation between the moments, Panel A of Table 2

comments in Dew-Becker (2021) who estimate realized monthly moments using 15-day maturity options to infer proxies for the expected moments.

reports the results of panel regressions of the form

$$\text{Realized moment}^i_{t,T} = \alpha^i + \beta \underbrace{E_t[\text{Moment}^i_{t,T}]}_{\text{Option implied}} + \epsilon^i_{t,T}. \tag{12}$$

where i represent the different stock market indexes. Panel A reports the results of two separate panel regressions. In the first panel regression, the first row, we pool the moments from all indexes and run the regression while including index fixed effects and clustering standard errors by time and country.[8] In the second panel regression, the second row, we first standardize the (standardized) moments within each index before we pool them together.[9] We make this small transformation because some indexes tend to have larger moments in absolute values than others and these indexes determine most of the variation in panel regression (i) and might drive the results. In the second panel regression, we clusters standard errors by country and time and include index fixed effects.

The first column of Panel A reports the slope coefficient of ex post realized skewness regressed on ex ante implied skewness. In both panel regressions, the slopes are 0.19, which are statistically significant at the 1% level with a t-statistic of 3.01 and 3.20 respectively. The adjusted R^2's are 3% to 15%. The results presented in the remaining columns of Panel A support the hypothesis that the conditional ex ante implied moments predict the conditional ex post realized moments. The results are even stronger at the quarterly horizon where the adjusted R^2 for skewness is as high as 35%.

Panel B of Table 2 reports the result of regression (12) for each stock market index individually. The index-wise results also support the hypothesis that ex ante implied moments predict ex post realized moments. The results are particularly strong for the US indexes, which is not surprising as these are the indexes where we have the richest option data and therefore are most confident in the estimated moments. All coefficients that are statistically significant support that implied moments predict realized moments positively. The index-wise regressions are statistically significant at the 10% level with positive slopes in 12/20 regressions for monthly skewness, 10/20 for monthly kurtosis, 16/20 for quarterly skewness, and 11/20 for quarterly kurtosis.

---

[8]Clustering by country or by index has little effect on our results. We choose to cluster by country rather than by index because the four US indexes might have correlated error terms.

[9]For example, before pooling the data for the second panel regression for realized skewness onto implied skewness, we standardized both the right and the left side as: $\text{Skewness}^{standardized}_{t,T} = (\text{Skewness}_{t,T} - mean(\text{Skewness}_{t,T}))/variance(\text{Skewness}_{t,T})^{1/2}$ where the mean and the variance of the skewness are the unconditional in-sample estimates for the realized or implied skewness respectively.

Overall, we conclude that there is a strong positive linear relation between the ex ante implied moments and the ex post realized moments, both in averages and in the time-series. Next, we use the moments to reveal new facts about the higher-moment risk of stock market returns.

3 Time Variation in Higher-Order Moments

This section studies time variation in the 3rd and 4th moment of the return distribution for stock markets around the world. Section 3.1 documents comovement among the higher-order moments over time. Section 3.2 documents cyclical fluctuations in the higher-order moments. Section 3.3 identifies a global component in higher-moment risk.

3.1 Time Variation and Comovement in Higher-Order Moments

Figure 3 shows the time series of the ex ante option implied skewness and kurtosis at the monthly and quarterly horizon for the S&P 500 stock market index. The skewness is negative on almost all days and kurtosis is often well above three. The conditional distributions is left skewed and fat tailed relative to the normal distribution. These results are consistent with the the well-known evidence from histograms of historical returns.

Figure 3 also shows that the skewness tends to be more negative at times when the kurtosis is more positive, suggesting that there are periods where both higher-order moments contribute to increased probability in the left tail of the return distributions. To formally document this between the higher-order moments, Panel A of Table 3 reports the slope coefficients of the panel regressions across the 20 stock indexes,

$$\text{Skewness}_{t,T}^i = \alpha^i + \beta \text{Kurtosis}_{t,T}^i + \epsilon_{t,T}^i \tag{13}$$

where i represent the different stock market indexes. Panel A of Table 3 reports the results of two panel regression where we. In the first regression we pool the moments of all the indexes and in the second we standardize the (standardized) moments within each index before pooling them. We include index fixed effects and cluster standard errors on country and time. We find a strong negative relation between skewness and kurtosis. For ex ante implied moments at the monthly horizon, the slope coefficients are statistically significant at the 1% level with a t-statistic of -8.97 and -16.24 and adjusted R^2's of 56% and 77% respectively. The results are similar for the quarterly horizon. The last six columns of Table

3 report the results when using ex post realized moments. We find a strong negative relation between skewness and kurtosis in the realized moments as well.

Panel B of Table 3 reports the results for the individual stock market indexes. Using implied or realized moments at the monthly or quarterly horizons, we find a strong negative relation between skewness and kurtosis in the time-series of individual indexes. The slopes are negative and statistically significant in 76 of the 80 regressions. The main outlier is in the Netherlands where skewness is positively related to kurtosis on the quarterly horizon (for the expected moments). In fact, if we exclude the Netherlands from our first Panel regression then the coefficient at the quarterly horizon for implied moments turns strongly significant with a t-stat of -15.69 and an adjusted R^2 of 81%.

3.2   Cyclical Fluctuations in Higher-Moment Risk

Figure 3 indicates that the higher-order moments vary with the state of the financial markets and the economy as a whole. For example, looking at subfigure 3b, we see that during the crisis in 2007-2009, the skewness approaches zero and the kurtosis approaches three, suggesting that the conditional distribution is close to normal. However, during good times, such as the periods leading up to the financial crisis, skewness drops substantially and kurtosis increases, indicating substantial risk in the higher-order moment of the return distribution. In this section, we formally study such cyclical fluctuations in higher-moment risk by linking the fluctuations to variables that capture good and bad times.

We first consider the relation between higher-moment risk and the variance. Figure 4 displays the time-series plots of the monthly and quarterly skewness along with the variances of the S&P 500 stock market index. Both for the monthly and the quarterly horizon, the two times series are positively correlated: skewness is more negative when variance is low. For instance, skewness is high (close to zero) during the burst of the tech bubble and during the financial crisis, during which variance is somewhat high. Conversely, skewness is most negative during the low variance period from 2004 to 2007 and the low variance period from 2012 and until 2020.

This positive relationship between variance and skewness is highly statistically significant as shown for monthly horizon in the first three columns of Panel A of Table 4 for ex ante implied moments and in Panel A of Table 5 for ex post realized moments. Panel A reports panel regressions on the form:

$$\text{Higher-order moment}_{t,T}^{i} = \alpha^{i} + \beta \text{Variance}_{t,T}^{i} + \epsilon_{t,T}^{i} \tag{14}$$

where "Higher-order moment$_{t,T}$" is either the conditional skewness or kurtosis and i denotes the different indexes. We report the results of two panel regressions: (i) in the first panel regression we pool the moments of all the indexes and (ii) in the second panel regression, we first standardize the (standardized) moments within each index before pooling them. We include index fixed effects and cluster standard errors on country and time. For implied moments at the monthly horizon, skewness is positively related to variance with slope coefficients of 0.08 and 0.37, t-statistic of 7.31 and 6.80, and adjusted R^2's of 0.30 and 0.13 for raw and standardize moments. The results for implied skewness are similar at the quarterly horizon as reported in columns seven to ten. In terms of implied kurtosis, we find a statistically significant and negative relationship with implied variance with a t-statistics from -6.61 to -8.12 at the monthly horizon and -3.22 to -5.39 at the quarterly horizon. For ex post realized moments, Panel A of Table 5 reports similar panel regression results as for the implied moments, however the statistical significance is slightly lower and the adjusted R^2s are also lower.

Panels B of Tables 4 and 5 report results from regression (14) at the individual index level using either the ex ante implied or the ex post realized moments. The overall picture for both implied and realized moments is that skewness is positively associated with variance and kurtosis is negatively associated with variance. The relationships are statistically significant with the positive sign for skewness and negative sign for kurtosis 16/20 to 19/20 indexes for ex ante implied moments and 12/20 to 17/20 indexes for ex post realized moments. Importantly, we find statistical significance for the US indexes in all but two regressions. The US results are particular interesting because these are the indexes for which we have the richest data and consequently are most certain about the estimated moments.

The regressions in Equation (14) impose a linear relation between the variance and higher-order moments, but the real relation is strongly non-linear. To illustrate the non-linearity, Figure 5 shows a scatterplot of the ex ante variance and skewness on of S&P 500. The skewness (y-axis) is a concave function of the variance (x-axis), increasing rapidly for low variance and more slowly for higher variance. We find no evidence for significant non-monotonicity, suggesting that skewness is always weakly increasing in variance. The same holds true when considering standard deviation instead of variance on the x-axis. None of the results presented throughout the paper are sensitive to this non-linearity. In Section 5, we study disaster-based asset pricing models and find that these tend to produce the same concave relation between skewness and variance.

The cyclical fluctuations documented in Tables 4 and 5 holds at both the monthly and

quarterly horizon. However, it is not clear from these regressions whether the strength of the cyclical fluctuations depend on the horizon of the returns. In Figure A1 in the Online Appendix, we document that they do, as the fluctuations are slightly stronger at the shorter horizon. This finding is consistent with the well known fact that conditional non-normality is weaker at longer horizons due to a central limit effect (see discussion in, e.g., Eraker, Johannes, and Polson 2003, Duffie and Pan 1997, or Das and Sundaram 1999).

We next study how higher-order moments vary with valuation ratios, which is a standard measure of good and bad times in the asset pricing literature (see, e.g., Campbell and Cochrane 1999). We measure valuation ratios using the country-level dividend-price ratio, with a high dividend-price ratio reflecting bad times in the given country at the given time. In Table 6, we report results of regressions of ex ante implied moments onto the contemporaneous dividend yield in the given country,

$$\text{Higher-order moment}_{t,T}^i = \alpha^i + \beta (D/P)_t^i + \gamma t + \epsilon_{t,T}^i. \tag{15}$$

We include time trend in the regressions to account for a potential trend in dividend yields and higher-order moments. Panel A again reports the results of two panel regressions. In the first regression, we pool the moments of all the indexes, and in the second regression, we first standardize the (standardized) moments within each index before pooling them. We find that ex ante implied skewness is less negative when the dividend-price ratios are higher (i.e., during bad times). Similarly, we find that kurtosis tends to be less positive when dividend-price ratios are higher. Panel B of Table 6 reports the results of regression (15) at the individual index level. The results are broadly consistent for the US and European indexes, that is, skewness becomes less negative when the dividend-price ratio goes up while kurtosis becomes less positive. Table 7 reports similar results for ex post realized moments.

Finally, we also consider cyclicality relative to three U.S.-specific measures of good and bad times. We find similar results using other measures of bad times. In particular, Table 8 reports U.S. results, in which we measure bad times based on the consumption-wealth ratio 'cay' from Lettau and Ludvigson (2001), the Chicago Fed national activity index 'CFNAI', and NBER recessions. Panel A reports the results for the cay variable. Here we regress the higher-order moments on cay, again including a time trend to account for trend in higher-order moments and cay over the sample. For both ex ante implied and ex post realized moments, we find strong and statistically significant relationships between cay and the subsequent higher-order moments. During periods where cay is low, i.e. good times with high wealth relative to consumption, the distribution is more left skewed and fat tailed. Panel

14

B reports the results for the CFNAI variable. During good times with more economic activity, as measured by CFNAI, the distribution is again more left skewed and fat tailed. Finally, Panel C reports the results for NBER recessions. During expansions, the distribution is more left skewed and fat tailed than during recessions. Taken together, these results emphasize the robustness of our results with respect to definitions of good and bad times.

3.3   The Global Factor Structure in Higher-Order Moments

This section documents a global component in higher-moment order of stock market index returns. For the purpose of this analysis, we estimate the principal components of the space spanned by moments of the international stock markets. For example, the first column of Panel A in Table 9 reports the coefficients of the first principal component of the space spanned by ex ante variances for the twenty stock market indexes. The first principal component of ex ante variance explains as much as 83% of the joint variation in variances across stock market indexes, which suggests that there is a strong common component in stock market variance around the world.

In column five of Panel A, we report the results of a similar analysis but for ex ante skewness. There is strong common component in the skewness across stock market returns around the world. The global skewness factor (the first principal component of the space spanned by the skewness of the twenty stock market indexes) explains 41% of the joint variation in skewness around the world. Similarly, column nine reports that the global kurtosis factor explains 43% of the joint variation in individual stock market kurtosis.

To further investigate if the individual index moments relate to the common factors, we regress the first principal component of the moment onto the moment of each index. For example, for skewness, we regress:

$$\text{Skewness}_{t,T}^i = \alpha^i + \beta^i \text{Skewness PC1}_{t,T} + \epsilon_{t,T}^i \tag{16}$$

where i indicates the indexes and Skewness $\text{PC1}_{t,T}$ is the first principal component of skewness for the twenty indexes. The sixth to eight columns of Panel A reports the results for skewness. The coefficients are positive in all regressions and statistically significant for 18/20 indexes. The adjusted R^2 are also high and typically range from 0.30 to 0.60. Columns two to four report results of similar index-wise regressions but for variance and columns ten to twelve investigate the regressions for kurtosis. Overall, the individual indexes load positively and statistically significant on the global moment factors.

Lastly, in Panel B of Table 9, we report the results when regressing the first principal component of skewness or kurtosis onto the first principal component of variance:

$$\text{Higher moment PC1}_{t,T} = \alpha + \beta \text{Variance PC1}_{t,T} + \epsilon_{t,T} \qquad (17)$$

where "Higher moment PC1$_{t,T}$" is either the first principal component of skewness or kurtosis. We find that the common skewness factor is positively related to the common variance factor. The slope of the regression is 0.54, which is statistically significant with a t-statistic of 10.40 and the adjusted R^2 is 0.59. Similarly, the global variance factor also explains a large fraction of the global kurtosis factor with a negative slope coefficient of -0.69, a t-statistic of -6.28, and an adjusted R^2 of 0.42.

These results suggests that there is strong global component in higher-moment risk and thus the shape of distribution of returns. The global component suggests that the variation in higher-moment risk we are uncovering is driven, to a large extent, by a global economic factor and not by market micro-structure issues or idiosyncratic trading patterns in individual countries.

4   Higher-Moment Risk and Conditional Tail Probabilities

The previous section documents strong cyclical variation in the shape of the distribution of stock returns. This variation influences the probability of tail events, or tail risk, which we study in this section.

It is useful to separate between two different types of tail risk. One measure of tail risk is the probability of an *unconditional* tail loss. This could, for instance, be the probability of observing a loss of 30% or more over the subsequent month (relative to the expected value). This probability is influenced by the variance of the distribution as well as the skewness, kurtosis, and other higher-order moments. We instead focus on the probability of a *conditional* tail loss. This is the probability of observing a loss of X conditional standard deviations. This measure nets out the effect of the standard deviation, which means that this probability is driven by higher-order moments.

In this section, we estimate time variation in such conditional tail loss probabilities. We do so in two ways. In Section 4.1, we extract the probabilities directly from option prices using Breeden and Litzenberger (1978). In Section 4.2, we extract the probabilities using

16

econometric techniques developed by Bollerslev, Todorov, and Xu (2015). In both settings, we find that probabilities of conditional losses are substantially elevated in good times when the distribution is more left skewed and fat tailed. The conditional tail-loss probabilities similarly drop in bad times.

These cyclical patterns in conditional tail-loss probabilities provide robustness to our findings on higher-moment risk in Section 3: across multiple ways of measuring tail loss probabilities, we consistently find evidence consistent with the distribution being more left skewed and fat tailed in good times. The tail loss probabilities also help flesh out the direct implications of our results for investors, regulators, and other economic agents. The results on tail loss probabilities, for instance, suggest that value-at-risk type estimates underestimate risk during good times, such as the run up to the global financial crisis. The results also suggest that volatility-managed portfolios – such as those studied by Moreira and Muir (2017) – are exposed to cyclical fluctuations in risk that is induced by variation in higher-order moments.

4.1 Conditional Tail Loss Probabilities from Option Prices

We first estimate conditional tail loss probabilities directly from option prices by using Breeden and Litzenberger (1978). We employ the same assumptions as in Section 2.1 and introduce the notation $D_{t,T}$ to capture the dividends paid on the risky asset between time t and time T. Using Breeden and Litzenberger (1978), we can write the risk-neutral expectation that returns are below a certain threshold as

$$P_t(R_{t,T} < \alpha) = R_{t,T}^f \text{put}'_{t,T}(\alpha S_t - D_{t,T}), \tag{18}$$

where $\text{put}'_{t,T}(\alpha S_t - D_{t,T})$ is the first derivative of the put option price with strike $\alpha S_t - D_{t,T}$.

Equation (18) shows that we can estimate the probability of tail losses by estimating the first derivative of put options. We discuss the empirical restrictions and considerations for the estimation of these first derivatives in Appendix B. Using equation (18), we estimate the probability of conditional tail losses. We define conditional tail losses as the probability of incurring a loss that is larger than 5 *conditional* standard deviations of returns. We consider risk-neutral standard deviations estimated as outlined in Section 2.1.

Figure 6 shows these tail probabilities estimated on the monthly horizon for the S&P 500. Figure 6a to the left shows the conditional probability in a solid blue line. The probability clearly declines during the global financial crisis and during the stock market draw-down of

the early 2000s. It also drops during March 2020 as the Covid crisis unfolds. On the other hand, the probability is substantially elevated during the seemingly calm periods of 2005-2007 and the end of the 2010s. For comparison, the figure also plots the probability of the loss according to the normal distribution (dashed line), which is close to 0 (and constant).

It is worth contrasting the procyclical behavior of the conditional tail loss probabilities to the behavior of the unconditional tail loss probabilities. To this end, Figure 6b shows in the blue solid line the *unconditional* probability of a -3 unconditional standard deviation event. At the monthly horizon, three unconditional standard deviations are approximately 18%. The probability of an unconditional tail loss of this size is greatly enhanced during bad times, such as the global financial crisis. The countercyclical variation in the unconditional tail loss probabilities is, as we shall see, driven by the countercyclical variation in volatility.

To better understand the role of volatility and higher-order moments, Figure 6b also plots the probability of the loss according to the normal distribution (dashed line). The shaded area between this line and the estimated probability is the part of the probability coming from higher-order moments. In many parts of the sample, higher-order moments constitute the majority of the probability of the 18% percent drop. However, most of the variation in tail risk comes from variation in the conditional volatility. The spike observed during the global financial crisis is, for instance, solely driven by a spike in the volatility. This result emphasizes that unconditional tail risk is mostly reflective of volatility and less so of higher-order moments.

In Figure 7a, we plot the conditional tail loss probabilities along with the skewness and kurtosis of the return distribution. The conditional tail loss probabilities are larger when the distribution is more left skewed and fat tailed. The correlations are -0.74 and 0.36, respectively. These results emphasize the importance of skewness and kurtosis for tail-loss probabilities.

4.2   Conditional Tail Loss Probabilities from a Parametric Approach

We next consider an alternative, parametric approach to estimating conditional tail-loss probabilities. We focus on the very up-to-date approach in Bollerslev, Todorov, and Xu (2015), but note that there is a long econometric literature using parametric methods to estimate statistical properties of stock returns (see, e.g., Pan 2002; Aït-Sahalia 2004; Eraker, Johannes, and Polson 2003; Bollerslev and Todorov 2011a; Christoffersen, Jacobs, and Ornthanalai 2012; Maheu, McCurdy, and Zhao 2013).

Bollerslev, Todorov, and Xu (2015) aims to estimate the impact of jumps on stock returns. They do so by specifying a functional form for the risk-neutral jump intensity and estimating the relevant parameters from the prices of out-of-the-money put and call options. In particular, the authors follow Bollerslev and Todorov (2014) and assume that the risk-neutral jump intensity process takes the form

$$v_t^Q(dx) = (\phi_t^+ \ e^{-\alpha_t^+ x} 1_{\{x > |k_t|\}} + \phi_t^- e^{-\alpha_t^- |x|} 1_{\{x < -|k_t|\}}), \tag{19}$$

where x refers to stock prices, α_t^+ and α_t^- are the parameters that control the rate of decay of the tails, and ϕ_t^+ and ϕ_t^- are "level shifts" in the intensity process. This functional form allows for a different shape of the left and right tails of return distribution, with the shapes being governed by the parameters α and ϕ. The authors estimate α_t^- and ϕ_t^- directly from the prices of deep out of money put options at time t. We describe how we compute the parameters in Appendix C.[10]

Given the functional form in equation (19) and estimates of α and ϕ, it is straightforward to calculate the probability of very large losses. In particular, the authors focuses on losses that are so far into the left tail that they cannot plausibly be impacted by the diffusive element of stock prices. The authors show that one can calculate tail loss probability of observing such a loss, which the authors denote the left jump intensity (LJI), as

$$LJI_t(k_t) = \int_{x < -|k_t|} v_t^Q(dx) = \phi_t^- e^{-\alpha_t^- |k_t|} / \alpha_t^-. \tag{20}$$

Figure 8 plots the conditional tail probabilities of losing more than 10 conditional standard deviations over the next week. We follow Bollerslev, Todorov, and Xu (2015) and use $k_t = 10\sigma_t$ to insure that the threshold is so far into the tail that the probabilities are not impacted by diffusive elements.[11] The figure shows that the tail probabilities increase during good times and decrease substantially during the global financial crisis.[12] Table A15 in the Appendix further document the procyclical properties of these tail probabilities.

For comparison, we also plot the conditional tail-probabilities estimated using the non-

---

[10]Replication code and a thorough description of the data is available from the Viktor Todorov and Torben Andersen website on tail risk: tailindex.com.

[11]As in Bollerslev, Todorov, and Xu (2015), for this exercise, we compute the conditional standard deviation as the normalized Black-Scholes at-the-money implied volatility.

[12]These probabilities are also plotted in Figure 1 subplot C in Bollerslev, Todorov, and Xu (2015). However, the authors do not mention the time variation in these probabilities, nor do they they relate the probabilities to cyclical fluctuations in the financial markets.

parametric approach in Section 4.2 (dashed blue line). These probabilities are not expected to be exactly the same as the non-parametric probabilities because these are for the monthly horizon and for $5\sigma_t$ losses. However, one would expect the two probabilities to be highly correlated, which the figure indeed confirms. The two probabilities track each other closely with a correlation of 0.77.

In Figure 9, we plot the conditional tail probabilities alongside the skewness and kurtosis of the distribution of returns. As expected, the tail probabilities are higher when the distribution is more left skewed and more fat tailed. Table A14 in the Appendix further corroborates this relation between the conditional tail probabilities from the parametric approach and the higher-order moments. The relations are consistent with the results in Section 3 and Section 4.2, and they emphasize the robustness of our findings across methodologies.

5   Higher-Moment Risk in Disaster Models

In this section, we relate our results to the predictions of models based on time-varying disaster risk. We are particularly interested in the class of models in which disasters are represented by negative jumps in prices or consumption. As a first step, we study simple jump diffusion models where disasters are represented as jumps in returns. We then study the asset pricing models models where disasters are represented as negative jumps in consumption. We end with simulation studies of the leading consumption-based disaster models by Gabaix (2012) and Wachter (2013) and with a study of how higher-order moments relate to risk premia.

One of our main points is that disaster models produce return distributions that are more left skewed and fat tailed when disaster risk is high. If pricing during bad times is driven by heightened disaster risk, as disaster models argue, we should therefore expect the distribution of returns to be more left skewed and fat tailed during bad times. However, returns almost follow a normal distribution during bad times, which questions whether these are indeed periods of elevated disaster risk. By extension, the findings question whether fluctuations in risk premia and asset prices are driven by fluctuations in disaster risk.

5.1   The Impact of Jumps on the Distribution of Returns

To understand how disasters influence the distribution of stock returns, it is useful to first understand how negative jumps in prices influence the shape of the distribution. To this end, we focus on the jump diffusion model by Merton (1976). Stock prices evolve according

to the process

$$\frac{dS_t}{S_t} = \alpha dt + \sigma dB_t + (e^x - 1)dN_t - \lambda E(e^x - 1)dt, \tag{21}$$

where B_t is a Brownian motion with diffusive variance σ^2 and N_t is a Poisson process with constant jump intensity λ. The Brownian motion B_t and Poisson process N_t are assumed to be independent. The jump size, x, is normally distributed with mean μ_x and variance σ_x^2. We assume that $\mu_x < 0$, such that jumps are negative on average.

In this model, variance and skewness are given by,

$$\text{Var}_{t,T}^{\text{Merton}} = (\sigma^2 + \lambda\mu_{x^2})(T - t) \tag{22}$$

$$\text{Skewness}_{t,T}^{\text{Merton}} = \frac{\lambda\mu_{x^3}}{(\sigma^2 + \lambda\mu_{x^2})^{3/2}\sqrt{T - t}} \tag{23}$$

where $\mu_{x^3} = 3\mu_x\sigma_x^2 + \mu_x^3 < 0$ and $\mu_{x^2} = \mu_x^2 + \sigma_x^2 > 0$.

A higher jump intensity (λ) and a more negative average jump size (μ_x) both lead to a higher variance, as seen from equation (22). They also lead to a more left skewed distribution, as long as the intensity and magnitude of jumps are not too large.[13] The same results hold when introducing time variation in the jump intensity and the diffusive volatility, as illustrated in Figure 10. This figure shows the relation between skewness and jump intensity for four different extensions of the jump diffusion model above (see Appendix D for details). In all extensions, higher jump intensity leads to a more left skewed distribution. There is a similar impact of jumps on kurtosis, which increases in jump intensity and jump size.

Reduced-form models in which disasters are represented as negative jumps in prices thus predict that higher disaster risk (measured as higher jump intensity or more negative jump size) is associated with a more left skewed and fat tailed distribution. However, most disaster models represent disasters as negative jumps in consumption, which we turn to in Section 5.2.

Before progressing with the consumption-based disaster models, it is worth highlighting the features needed to explain the data in the simple reduced-form framework. One straightforward way of generating the key relation between skewness and variance is through a jump

---

[13]Skewness decrease in λ if $2\sigma^2 - \lambda\mu_{x^2} > 0$. This is true if jumps are infrequent and if the average jump size and variance is not too large. If jumps happen all the time (λ is very large) then the distribution will shift to the left and be "centered" around the mean of the jump distribution. In this case, the diffusive part will drive up the skewness of the distribution when the jump intensity increases. This concern is unlikely to apply for empirically relevant specifications of jump diffusion models.

diffusion model that has stochastic volatility and constant jump intensity and i.i.d. distribution of jump sizes. This model generates a distribution that is more negatively skewed when the volatility is higher. We illustrate this finding in Figure 11, which shows skewness as a function of volatility for one specification of such a model. Intuitively, the skewness is a product of two opposing forces: the negative jumps push towards a more left skewed distribution while the diffusive volatility push towards a more symmetric distribution. When diffusive volatility is elevated, the diffusive volatility plays a relatively larger role and the distribution thus becomes more symmetric. On the other hand, when diffusive volatility is very low, the jump component plays a relatively larger role and the distribution thus becomes more left skewed.

Previous work on jump-diffusion models suggests that such a model with stochastic volatility and constant jumps indeed fit stock returns well (Eraker, Johannes, and Polson 2003). The variation in skewness that we uncover is thus consistent with findings of the previous literature based on jump diffusion models. The results are, however, inconsistent with disaster-based models of asset pricing, as we emphasize in the next two subsections.

5.2 Disasters as Jumps in Consumption

Disaster-based asset pricing models introduce disasters as negative jumps to consumption. Wachter (2013), for instance, models consumption, C_t, as following the stochastic process

$$\frac{dC_t}{C_{t^-}} = \mu dt + \sigma dB_t + (e^{Z_t} - 1)dN_t, \tag{24}$$

where B_t is Brownian motion, μ and σ are the (constant) mean and diffusive volatility of the consumption process, and N_t is a Poisson process with time-varying intensity λ_t. The intensity λ_t is the probability of a disaster and evolves according to a CIR process driven by the Brownian motion $B_{\lambda,t}$. The shocks B_t, $B_{\lambda,t}$, and N_t are all independent. The size of the jump, or disaster, Z_t follows a time-invariant process and is assumed to be negative throughout.

Assuming a continuous time equivalent of Epstein-Zin preferences and modelling dividends as levered claims to consumption ($D_t = C_t^\phi$), Wachter shows that stock prices follow the following jump diffusion process,

$$\frac{dS_t}{S_{t^-}} = \mu_{S,t}dt + \sigma_{S,t}[dB_t \ dB_{\lambda,t}]^\top + (e^{\phi Z_t} - 1)dN_t, \tag{25}$$

where $\mu_{S,t}$ is the drift of the process and the diffusive volatility $\sigma_{S,t} = [\phi\sigma \; F(\lambda_t)]$ is a vector of the scaled consumption volatility and a non-linear function of the disaster intensity, $F(\lambda_t)$.

Time variation in the distribution of stock prices is driven by time variation in the disaster intensity λ_t. A higher disaster probability shows up as a negative jump in stock prices because it generates a negative jump in dividends (the jump in consumption scaled by the leverage factor ϕ). However, the higher disaster intensity also increases the diffusive volatility. The reason is that fluctuations in disaster probabilities influence stock prices even absent jumps, and this effect shows up in the diffusive volatility. Since the fluctuations in disaster probabilities is larger when disaster probabilities themselves are larger (recall that the disaster probability follows a CIR process), the diffusive volatility increases as disaster probabilities increase.

Since a higher disaster probability leads to a higher jump intensity in prices, there is a natural mechanism through which the return distribution becomes more left skewed when disaster probability increases (i.e., the effect of jumps on skew as per the discussion in Section 5.1). A higher disaster probability also increases the diffusive variance which, everything else equal, would lower the skewness of the return distribution (see equation (23)). However, as long as the impact of disaster risk on the diffusive volatility is not too large relative to the impact on the jump intensity, the effect on the jump intensity dominates and higher disaster probability leads to more left skewed distributions. In the upcoming section, we show that this second effect indeed dominates in leading disaster-based models, which is to say that higher disaster probability leads to more volatile and left skewed distributions.

It is important to emphasize that higher disaster risk does not only lead to a more left skewed and fat tailed distribution, it also leads to a higher volatility of returns. In the above framework, it does so through two channels. First, the higher disaster risk leads to a higher jump intensity in returns in equation (25), which leads to higher volatility (see equation 22). Second, the higher disaster risk also leads to higher more diffusive volatility, which similarly increases volatility. An increase in disaster risk thus makes the distribution more left skewed and more volatile. In Section 5.4, we further elaborate on how skewness and kurtosis on their own are incomplete measures of disaster risk when not accompanied by volatility.

The goal of most disaster models is ultimately to explain expected stock returns. In the consumption-based disaster models considered next, the equity premium increases when disaster risk increases. Periods with high disaster risk are thus bad times. The relation between disaster risk and risk premia ultimately lead to a strong relation between the equity premium and higher order moments, which we will explore in Section 5.4.

5.3 Higher-Moment Risk in Leading Disaster-Based Models

To get more precise results, we study the behavior of higher-order moments in simulation studies of the leading disaster-based models by Gabaix (2012) and Wachter (2013). In both models, higher disaster risk leads to a distribution of returns that is both more left skewed and more volatile.

The Disaster Model by Wachter (2013). In the disaster model by Wachter (2013), there is a time-varying disaster probability that gives rise to time variation in expected returns as well as the distribution of stock returns. In particular, higher disaster risk leads to: (1) higher expected returns and (2) a more left skewed and volatile return distribution.

We illustrate these results through simulation studies of the model. In Figure 12, we plot the first four moments of stock returns as a function of the disaster intensity λ. A higher disaster risk leads to higher expected returns and volatility. These two observations in isolation support the narrative that the increase in expected return and volatility that we tend to observe during bad times are driven by an increase in disaster risk. However, the model also predicts that the distribution of returns should become more left skewed when disaster risk increases, which runs counter to the cyclical fluctuations in higher-order moments documented in Section 3.

The above results follow naturally from equation (24) and (25) in Section 5.2. The higher disaster intensity leads to higher volatility through the impact on the diffusive volatility as well as the jump intensity. The higher disaster risk also generates a left skew because of the increased jump intensity.

More generally, the variance and skewness of the return distribution are negatively correlated in the model. The negative correlation is a natural product of the dynamics outlined above. The negative correlation is plotted in Figure 13, which shows the average realized skewness and volatility for different buckets of ex ante disaster intensity.[14] When the disaster intensity is low, the volatility is low and skewness is relatively higher (more right skewed); when disaster intensity is high, the volatility is high and the distribution is more left skewed. (The skewness is positive for most values of the disaster intensity; the positive average arises from the log-normal properties of the diffusive element in stock prices, which pushes towards a right skew on average.) The negative correlation between volatility and skewness runs counter to the results documented in the previous sections.

---

[14]We exclude buckets with very low probability of disaster. For the very low disaster probabilities, the distribution becomes close to log-normal and therefore skewness therefore increases in volatility given the properties of the log-normal distribution.

The Disaster Model by Gabaix (2012). In the disaster model by Gabaix (2012), there is time-varying resilience of the economy towards disasters. The probability of a disaster is assumed to be constant in the main calibration. A higher disaster risk, measured as a lower resilience towards disasters, again leads to a more left skewed, fat tailed, and volatile distribution of returns. It also leads to higher expected returns, conditional on the disaster being averted.

We illustrate the results for the higher-order moments through simulation studies in Figure 14. We simulate the model following the procedure in the paper and calculate option-implied volatility, skewness, and kurtosis (see Appendix E.2 for detail). In the two top figures, we plot skewness and kurtosis against volatility. A higher volatility is associated with more left skew and kurtosis. To understand these relations, note that the variation in all three moments is driven by time variation in the resilience towards disasters. When this resilience is low, the expected negative jump in stock prices coming from a disaster is larger (more negative), which increases the volatility and kurtosis and makes the distribution more left skewed.

Periods with low resilience towards disasters are also periods where stock prices are depressed (i.e., bad times, in our previous terminology). Combined with the dynamics discussed above, this fact gives rise to strong relations between the dividend-price ratio of the market portfolio and the higher-order moments. The two figures in the bottom of Figure 14 illustrate these relations. A higher resilience leads to a lower dividend-price ratio and a more left skewed distribution of returns. It also leads to a higher kurtosis. This finding illustrates how the distribution becomes more left skewed and fat tailed in bad times, which runs counter to the results in our empirical section.

5.4   Higher-Moment Risk and Expected Returns

As discussed above, the shape of the return distribution and the equity premium both vary over time with disaster risk. When disaster risk is high, the distribution of returns is more left skewed and volatile and the equity premium is higher. We should therefore expect skewness and volatility to predict future realized returns.

In Table 10, we explore this relation in theory as well as in the data. We first study how future realized returns relate to the ex ante skewness in the model by Wachter. Through simulations, we estimate slope coefficients for predictive regressions of realized returns on ex ante skewness (see Appendix E.1 for details). We run 40,000 simulations of 300 months length (25 years) and estimate median values and standard errors based on the simulations.

The leftmost columns of Table 10 shows that realized returns are higher when skewness is more negative (i.e., the distribution is more left skewed). We normalize skewness, so the slope coefficients imply that a one standard deviation increase in skewness increases the expected return next month by around 70 basis points, which is a large effect. The economic significance can similarly be seen from the R^2 of around 1%, which is high for monthly returns. The effect is, however, statistically insignificant given the short sample of 25 years.

In the next two columns, we report results from similar regressions in our data. We regress future realized stock returns on ex ante skewness in a panel consisting of the 17 countries included in our sample (see Table 1). We include country fixed effects and we cluster the standard errors across country and time. We again see a negative relation between skewness and expected returns. The effect is economically meaningful, although weaker than in the Wachter model, as risk premia increase by 20 to 27 basis points when skewness increases by one standard deviation. The effect is statistically insignificant, but this is consistent with our simulation study, which shows that the effect of skewness on returns is too weak to be detected in a 25-year sample. (In principle, the panel gives us a power gain relative to the single-country regressions in column 1 and 2; but this gain is very limited given the strong factor structure in returns and higher-order moments documented in Section 3.3.)

Risk premia are not driven by skewness alone but may also be influenced by the volatility of returns. In Wachter (2013), skewness and volatility are very highly correlated, as both are driven by the same underlying state variable (disaster intensity). Including volatility in the predictive regressions will therefore not improve the predictive ability of the model by much. In practice, however, Section 3.1 documents that although skewness and volatility are highly correlated, they are far from perfectly correlated. Including volatility in the predictive regressions could thus be relevant. The regressions in column 5 and 6 do so. The inclusion of volatility slightly increases the slope coefficients on skewness and it becomes statistically significant in the regressions that are using raw returns. The p-value for the slope coefficient for excess returns is 0.11.

Overall, the results above are consistent with the idea that skewness captures a risk for which investors want to be compensated. The results emphasize the relevance of understanding the cyclical behavior of skewness (and other higher-order moments) and it lends further support to the idea that disaster risk is priced in financial markets (see also Harvey and Siddique (2000)).

6   Conclusion

We document new facts about time variation in the higher-order moments of the distribution of stock returns. We show that the return distribution for the market is more left skewed and fat tailed during good times than during bad times. This pattern holds across the 17 countries we study in our sample, across multiple measures of higher-order moments, and across many definitions of good and bad times.

This new result is surprising given our knowledge about tail risk. Indeed, tail risk, defined as the probability of losing a fixed percentage on your portfolio, tends to increase during bad times where variance is high (Kelly and Jiang, 2014; Bollerslev and Todorov, 2011b). Given this finding, one might conjecture that the return distribution is more left skewed and fat tailed during bad times, but we show that the opposite is the case. Rather, the increase in tail risk we observe during bad times comes from the fact that the variance of the return distribution increases, with the higher-order moments moving in way that reduces overall tail risk.

When looking at conditional tail risk, we document tail probabilities that strongly procyclical. During bad times, the probability of a 5-sigma loss is highly elevated, given the left skewed and right tailed distribution. But during the global financial crisis, however, the probability of a 5-sigma loss is substantially dampened, and close to that predicted by a normal distribution.

The fact that higher-moment risk disappears during bad times is hard to reconcile with the notion that disaster risk is elevated during these periods. We show that, according to standard asset pricing models, higher disaster risk should be associated with more higher-moment risk, in the sense that the distribution of return should be more left skewed and more fat tailed. The fact that we see the opposite in the data questions whether disaster risk is truly elevated during bad times, and by extension, whether counter-cyclical variation in risk premia and valuation ratios is driven by time-varying disaster risk. These results echo recent findings by Baron, Xiong, and Ye (2023), who argue that disaster risk is not elevated during periods that the asset pricing literature refers to as bad times.

References

Andersen, Torben G., and Oleg Bondarenko, 2007, Construction and interpretation of model-free implied volatility, *Working paper*.

Aït-Sahalia, Yacine, 2004, Disentangling diffusion from jumps, *Journal of Financial Economics* pp. 487–528.

Bae, Kwangil, and Soonhee Lee, 2021, Realized higher-order comoments, *Quantitative Finance* 21, 421–429.

Bakshi, Gurdip, Nikunj Kapadia, and Dilip Madan, 2003, Stock return characteristics, skew laws, and the differential pricing of individual equity options, *Review of Financial Studies* 16, 101–143.

Bakshi, Gurdip, and Dilip Madan, 2000, Spanning and derivative-security valuation, *Journal of Financial Economics* 55, 205–238.

Bali, Turan, Beyong-Je An, Andrew Ang, and Nusret Cakici, 2014, The joint cross section of stocks and options, *Journal of Finance* 69, 2279–2337.

Bali, Turan, and Scott Murray, 2013, Does risk-neutral skewness predict the cross-section of equity option portfolio returns?, *Journal of Financial and Quantitative Analysis* 48, 1145–1171.

Baron, Matthew, Wei Xiong, and Zhijiang Ye, 2023, Measuring time-varying disaster risk: An empirical analysis of, *Princeton University Working Paper*.

Barro, Robert J, 2006, Rare disasters and asset markets in the twentieth century, *The Quarterly Journal of Economics* 121, 823–866.

Bollerslev, Tim, George Tauchen, and Hao Zhou, 2009, Expected stock returns and variance risk premia, *The Review of Financial Studies* 22, 4463–4492.

Bollerslev, Tim, and Viktor Todorov, 2011a, Estimation of jump tails, *Econometrica* 79, 1727–1783.

Bollerslev, Tim, and Viktor Todorov, 2011b, Tails, fears and risk premia, *Journal of Finance* 66, 2165–2211.

Bollerslev, Tim, and Viktor Todorov, 2014, Time-varying jump tails, *Journal of Econometrics* pp. 168–180.

Bollerslev, Tim, Viktor Todorov, and Lai Xu, 2015, Tail risk premia and return predictability, *Journal of Financial Economics* 118, 113–134.

Breeden, Douglas T., and Robert H. Litzenberger, 1978, Prices of state-contingent claims implicit in option prices, *The Journal of Business* 51, 621–651.

Campbell, John Y, and John H Cochrane, 1999, By force of habit: A consumption based explanation of aggregate stock market behavior, *Journal of Political Economy* 107, 205–251.

Christoffersen, Peter, Kris Jacobs, and Chayawat Ornthanalai, 2012, Dynamic jump intensities and risk premiums: Evidence from sp500 returns and options, *Journal of Financial Economics* pp. 447–472.

Das, Sanjiv, and Randarajan Sundaram, 1999, Of smiles and smirks: A term structure perspective, *Journal of Financial and Quantitative Analysis* 34, 211—-240.

Dew-Becker, Ian, 2021, Real-time forward-looking skewness over the business cycle, *working paper*.

Dew-Becker, Ian, and Stefano Giglio, 2023, Risk preferences implied by synthetic options, *National Bureau of Economic Research*.

Duffie, Darrell, and Jun Pan, 1997, An overview of value at risk, *Journal of Derivatives* pp. 7—-49.

Dumas, Bernard, Jeff Fleming, and Robert E. Whaley, 1998, Implied volatility functions: Empirical tests, *Journal of Finance* 53, 2059–2106.

Eraker, Bjørn, Michael Johannes, and Nicholas Polson, 2003, The impact of jumps in volatility and returns, *The Journal of Finance* 58, 1269–1300.

Gabaix, Xavier, 2012, Variable rare disasters: An exactly solved framework for ten puzzles in macro-finance, *Quarterly Journal of Economics* 127, 645–700.

Giglio, Stefano, Bryan Kelly, and Seth Pruitt, 2016, Systemic risk and the macroeconomy: An empirical evaluation, *Journal of Financial Economics* 119, 457–471.

Harvey, Campbell R., and Akhtar Siddique, 2000, Conditional skewness in asset pricing tests, *The Journal of Finance* 55, 1263—-1296.

Jiang, Lei, Ke Wu, Guofu Zhou, and Yifeng Zhu, 2020, Stock return asymmetry: Beyond skewness, *Journal of Financial and Quantitative Analysis* pp. 357–386.

Kelly, Bryan, and Hao Jiang, 2014, Tail risk and asset prices, *The Review of Financial Studies* 27, 2841–2871.

Lettau, Martin, and Sydney Ludvigson, 2001, Consumption, aggregate wealth, and expected stock returns, *The Journal of Finance* 56, 815–849.

Maheu, John M., Thomas H. McCurdy, and Xiaofei Zhao, 2013, Do jumps contribute to the dynamics of the equity premium?, *Journal of Financial Economics* pp. 457–477.

Merton, Robert C, 1976, Option pricing when underlying stock returns are discontinuous, *Journal of Financial Economics* 3, 125–144.

Moreira, Alan, and Tyler Muir, 2017, Volatility-managed portfolios, *The Journal of Finance* 72, 1611–1644.

Muir, Tyler, 2017, Financial crises and risk premia, *The Quarterly Journal of Economics* 132, 765–809.

Neuberger, Anthony, 2012, Realized skewness, *The Review of Financial Studies* 25, 3423–3455.

Pan, Jun, 2002, The jump-risk premia implicit in options: evidence from an integrated time-series study, *Journal of Financial Economics* 63, 3–50.

Tsai, Jerry, and Jessica A Wachter, 2015, Disaster risk and its implications for asset pricing, *Annual Review of Financial Economics* 7, 219–252.

Wachter, Jessica A., 2013, Can time-varying risk of rare disasters explain aggregate stock market volatility?, *The Journal of Finance* 68, 987–1035.

Zhen, Fang, and Jin E Zhang, 2020, Dissecting skewness under affine jump-diffusions, *Studies in Nonlinear Dynamics Econometrics* 24.
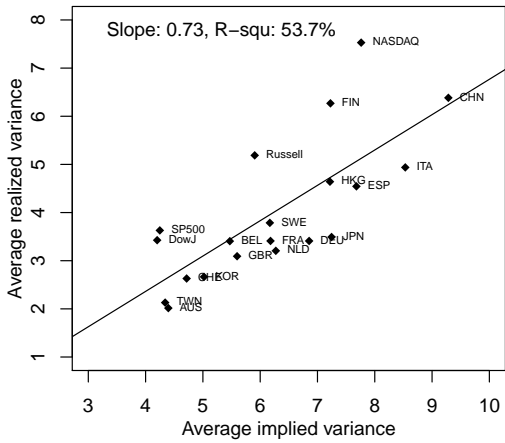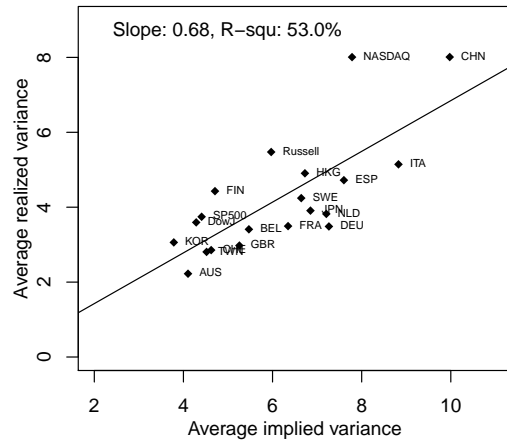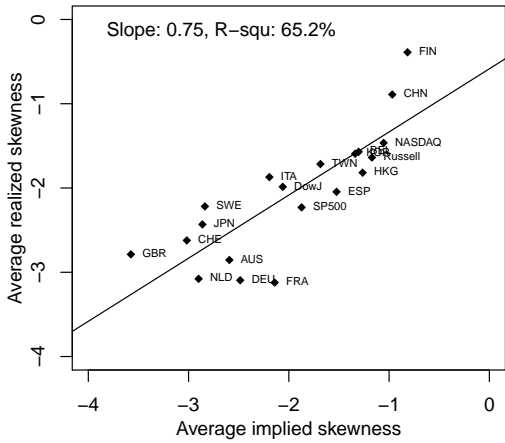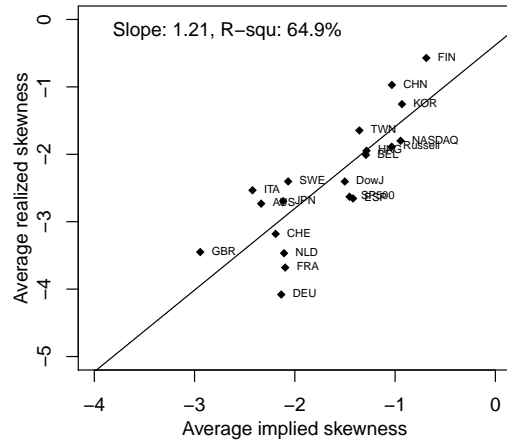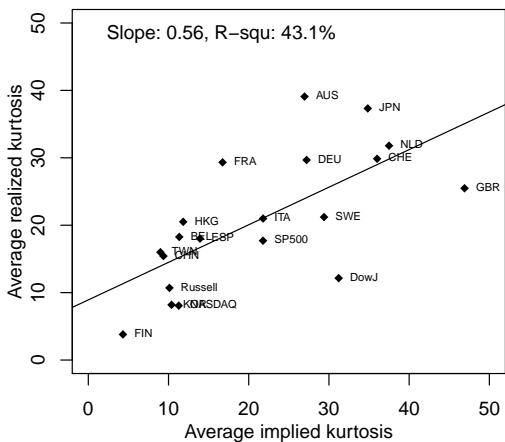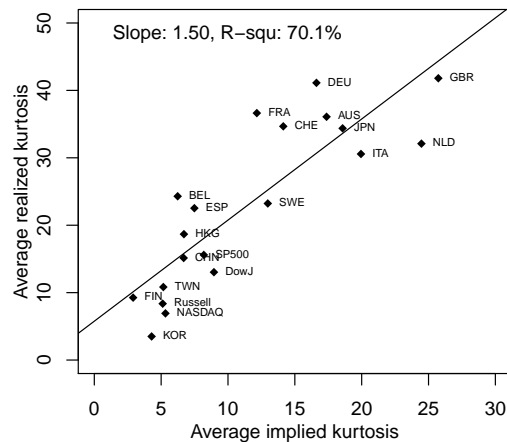
Figure 2: **Average Implied and Average Realized Stock Market Moments.** The figure shows the average time-series values of the option implied moments plotted against the average time-series values of the realized moments.

31
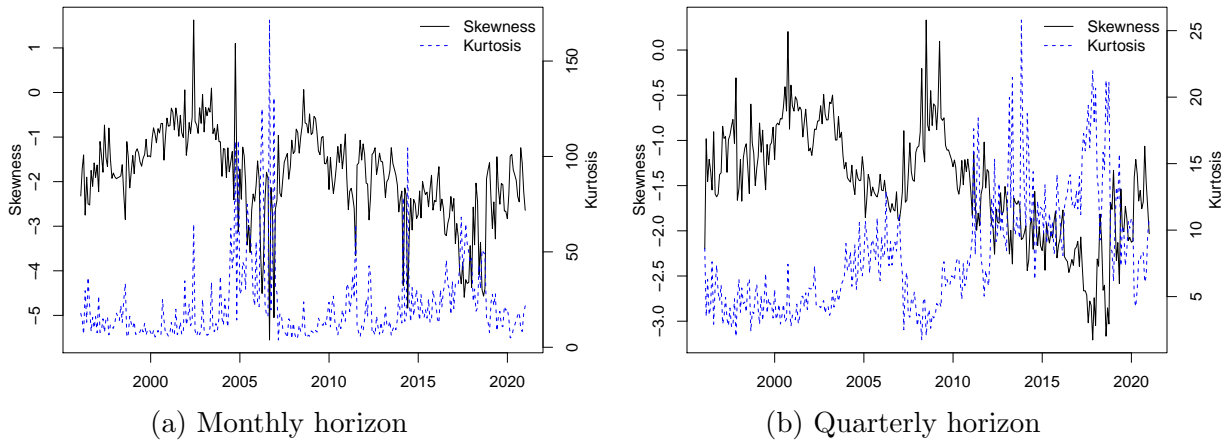
Figure 3: **Ex ante stock market skewness and kurtosis.** The figures show time series plots of monthly and quarterly horizon ex ante implied skewness and the ex ante implied kurtosis for the S&P 500 index.
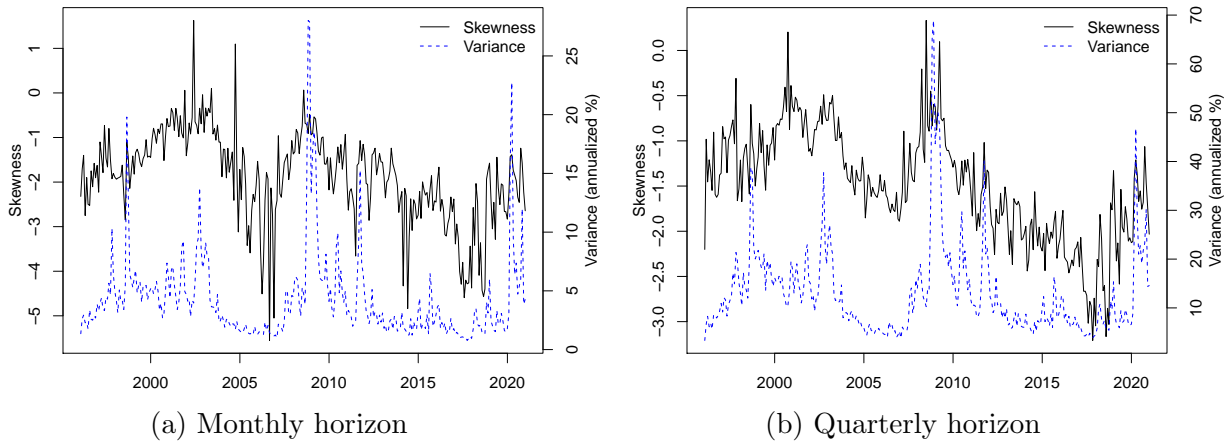
Figure 4: **Ex ante stock market skewness and variance.** The figures show time series plots of monthly and quarterly horizon ex ante implied skewness and the ex ante implied variance (annualized %) for the S&P 500 index.
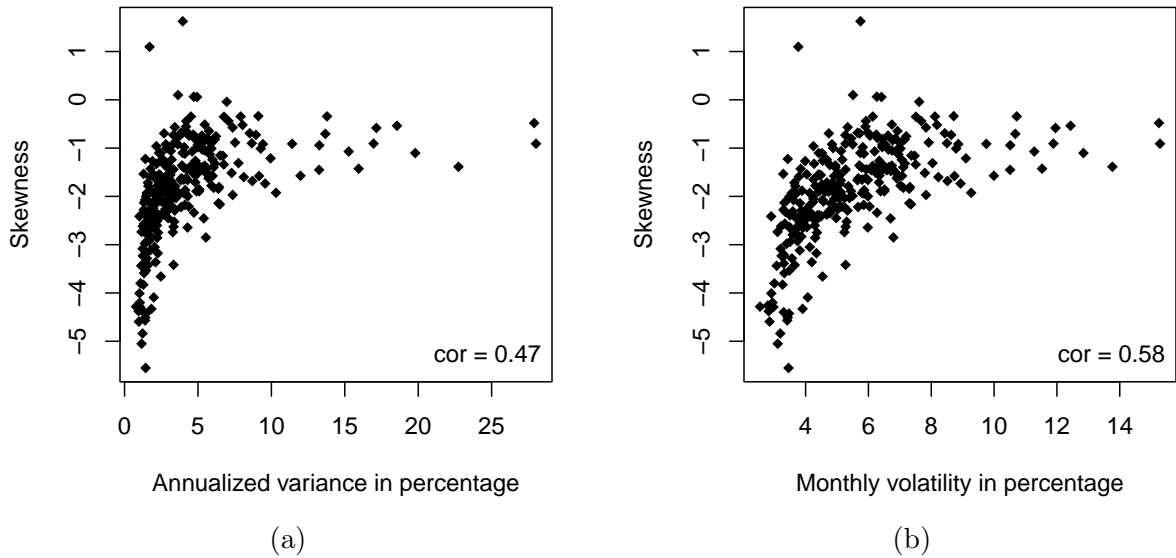
Figure 5: **Non-linear relation between higher-moment risk and variance.** The figures show scatterplots of monthly horizon ex ante skewness and ex ante variance (a) or volatility (b) for the S&P 500 index.

(a) Conditional left tail probabilities

(b) Unconditional left tail probabilities
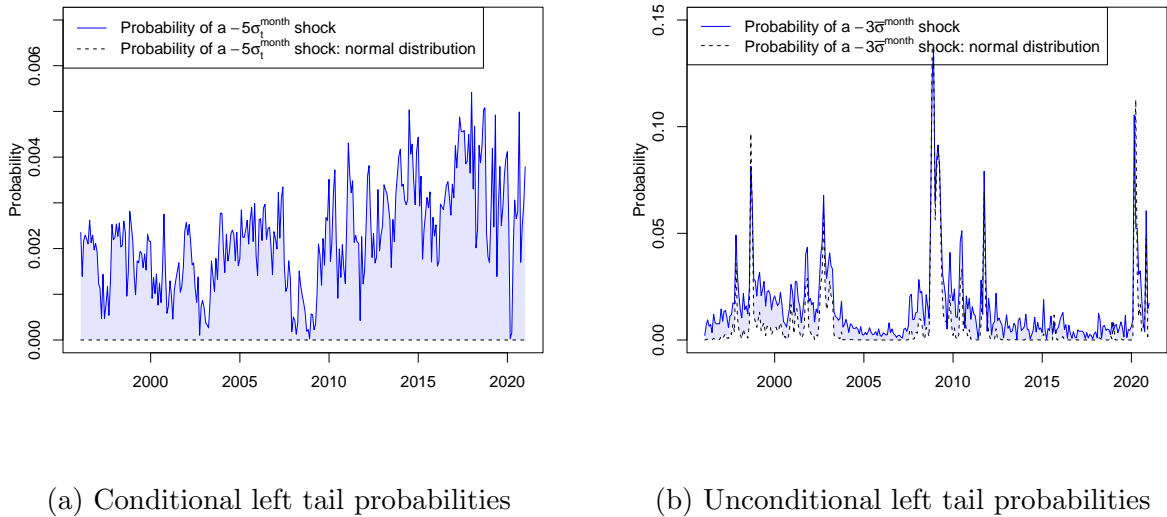
Figure 6: **Conditional and unconditional left-tail probabilities.** The figures show time series plots for the S&P 500 index of the end of month and monthly horizon left-tail probabilities. Subfigure (a) shows conditional probabilities of a -5 conditional standard deviation event and subfigure (b) shows the unconditional probability of a -3 unconditional standard deviation event, which is a -17.85% event. The probabilities are computed using the methods described in Section 4.1.
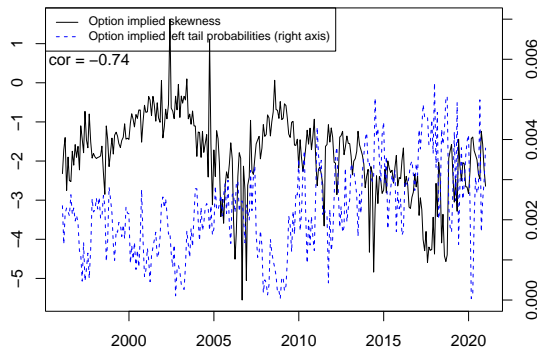
(a) Skewness
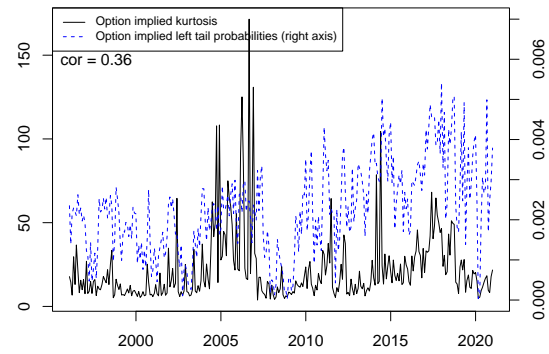
(b) Kurtosis

Figure 7: **Higher order moments and conditional left-tail probabilities.** The figures show time series plots of the S&P 500 monthly horizon ex ante skewness and kurtosis up against the ex ante probabilities of a -5 conditional standard deviation event computed from option prices as described in Section 4.1.
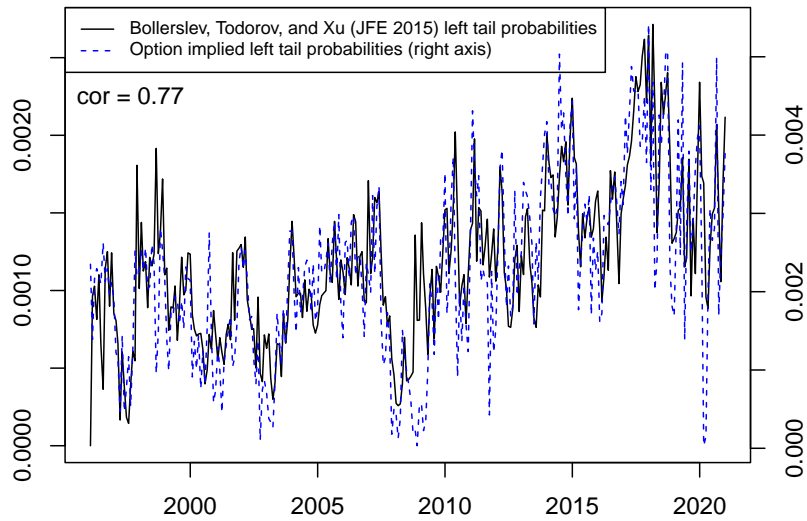
Figure 8: **Left-tail probabilities and jump tail probabilities.** The figure shows the option-implied −5 conditional standard deviation probability computed using the methods described in Section 4.1 and the within month average daily left-tail probabilities of weekly horizon "large" jumps in the Bollerslev, Todorov, and Xu (2015) jump diffusion model. We fix a "large" jump to be a −10 Black-Scholes at-the-money implied volatility shock. Both probabilities are for the S&P 500 index.
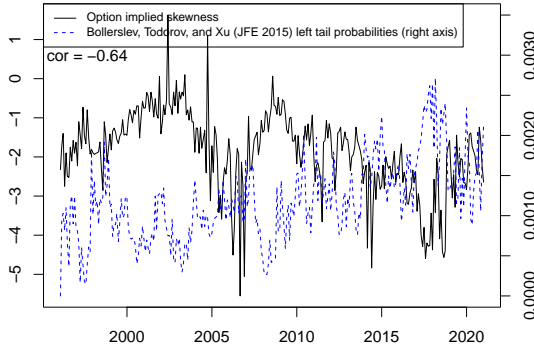
(a) Skewness
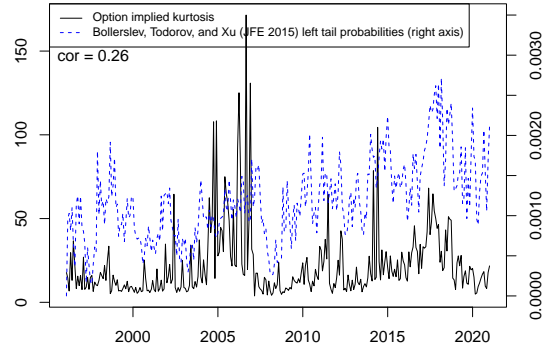
(b) Kurtosis

Figure 9: **Higher order moments and conditional jump tail probabilities.** The solid black lines in the subfigures is the end of month and monthly horizon ex ante skewness or kurtosis for the S&P 500 index. The dashed blue lines are the within month average left-tail probabilities of weekly horizon "large" jumps in the Bollerslev, Todorov, and Xu (2015) jump diffusion model. We fix a "large" jump to be a -10 Black-Scholes at-the-money implied volatility shock.
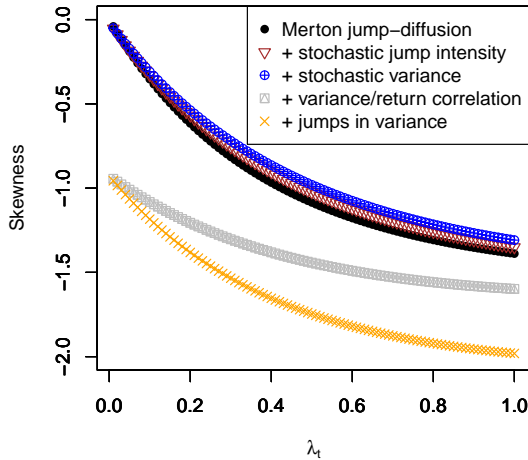
(a) Jump intensity
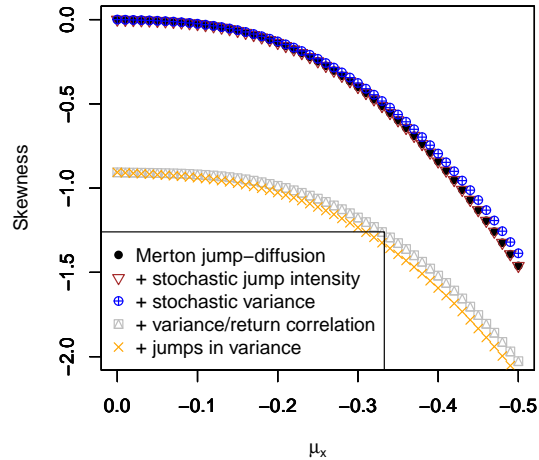
(b) Average jump size (reversed axis)

Figure 10: **Skewness in jump diffusion models.** The figure shows model implied skewness as a function of the jump intensity (a) or the average jump size (b) in various jump diffusion models of increasing complexity. We describe parameter values and computation in Appendix D. In solid black are the skewness for the Merton jump diffusion model. In brown square are the skewness for the Merton model augmented with stochastic jump intensity in returns. In blue diamond are the skewness from the "brown" model augmented with stochastic diffusive variance. In grey square, we augment the "blue" model with a non-zero correlation between returns and diffusive variance. In orange cross, we augment the "grey" model with jumps in variance.

36
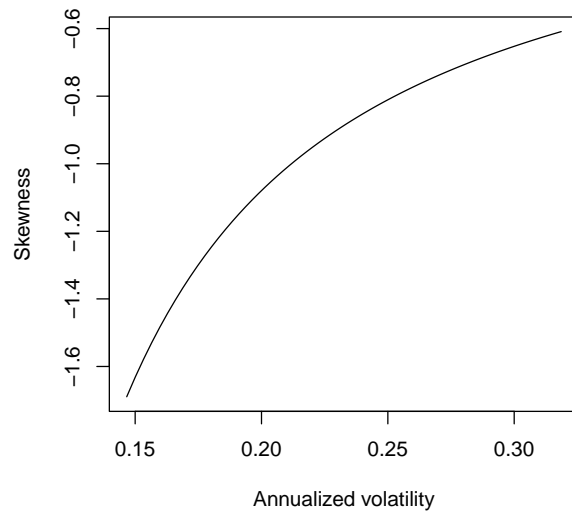
Figure 11: **Skewness and variance in an SVJ model.** This figure shows the skewness and variance in a stochastic volatility model with jumps in returns. The parameters are set as in Appendix D.
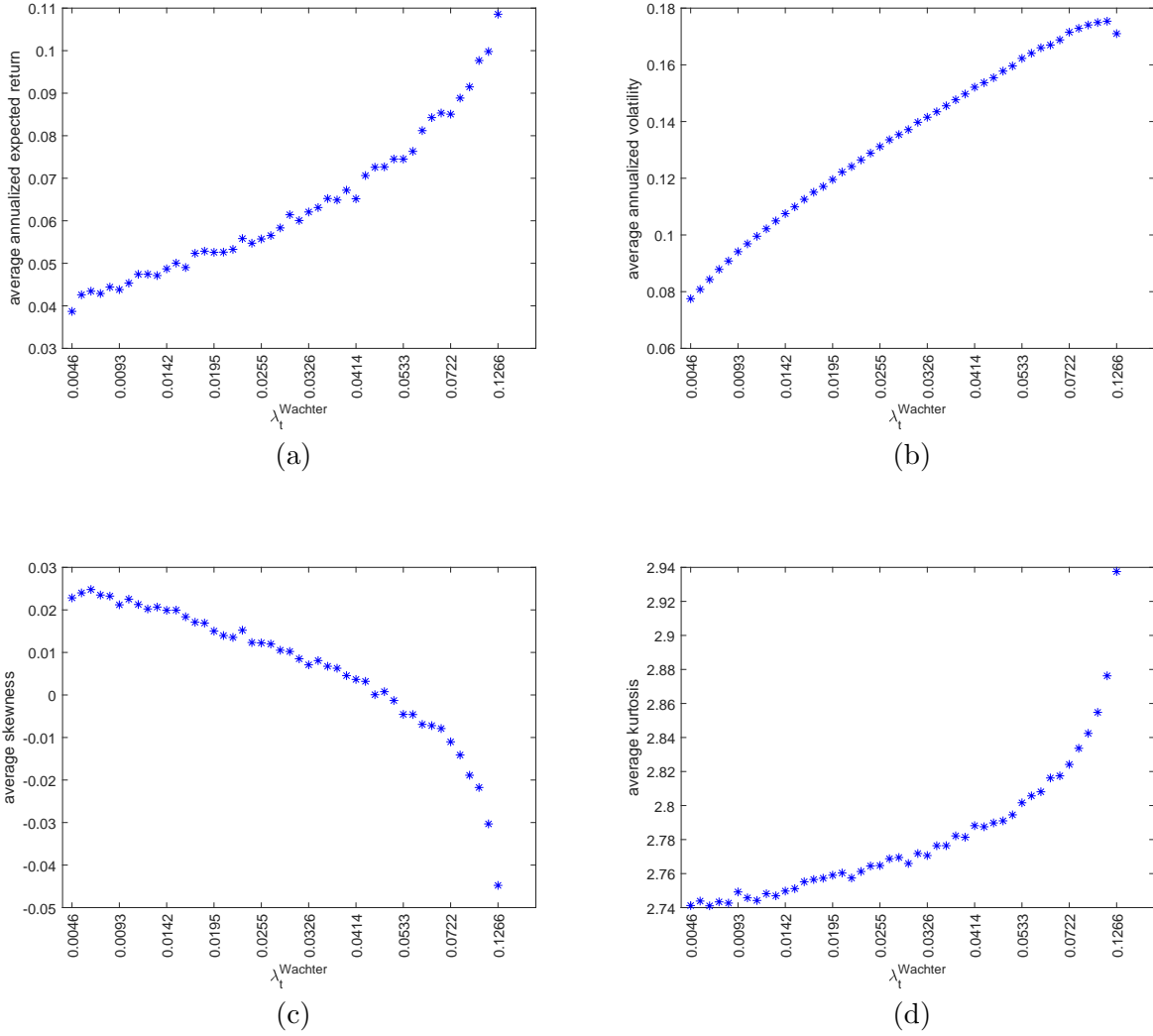
Figure 12: **Market return moments and the jump intensity in Wachter (2013).** Panel (a) shows a scatterplot of average simulated stock market expected returns for different values of the jump intensity, $\lambda_t^{\text{Wachter}}$. Panel (b) shows a scatterplot of average simulated stock market volatility for different values of the jump intensity. Panel (c) shows a scatterplot of average simulated stock market skewness for different values of the jump intensity. Panel (d) shows a scatterplot of average simulated stock market kurtosis for different values of the jump intensity. Simulation details are in Appendix E.1.
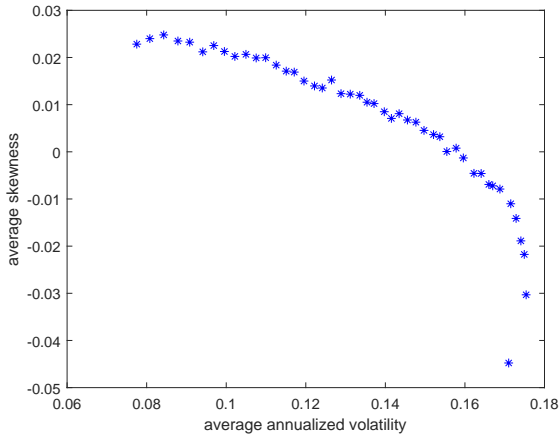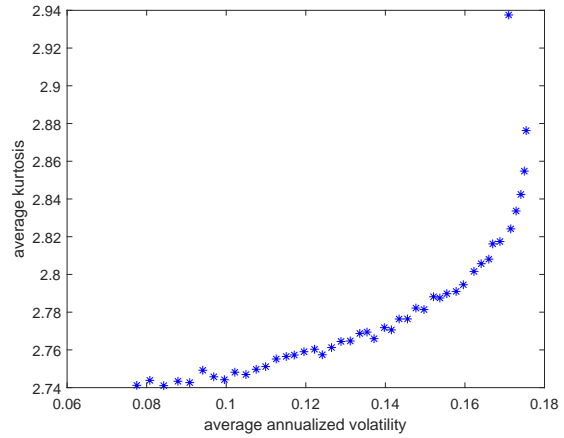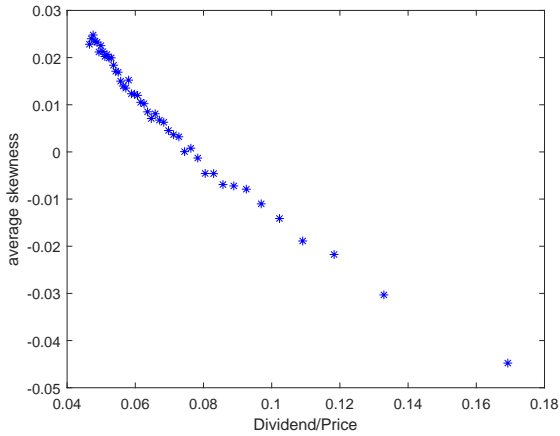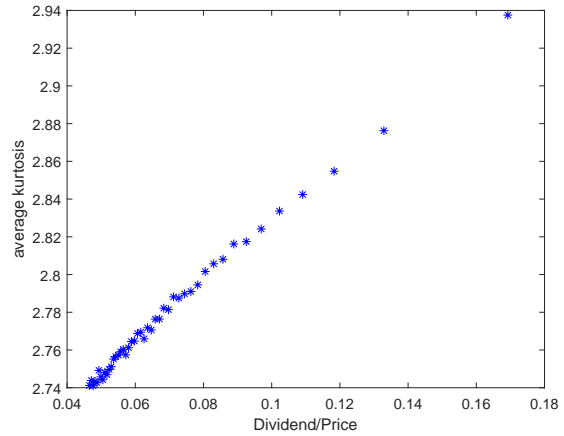
Figure 13: **Higher-moment risk, volatility, and dividend/price ratios in Wachter (2013).**
Panel (a) shows a scatterplot of simulated stock market skewness and volatility. Panel (b) shows
a scatterplot of simulated stock market kurtosis and volatility. Panel (c) shows a scatterplot of
simulated stock skewness and the dividend/price ratio. Panel (d) shows a scatterplot of simulated
kurtosis and the dividend/price ratio. Simulation details are in Appendix E.1.
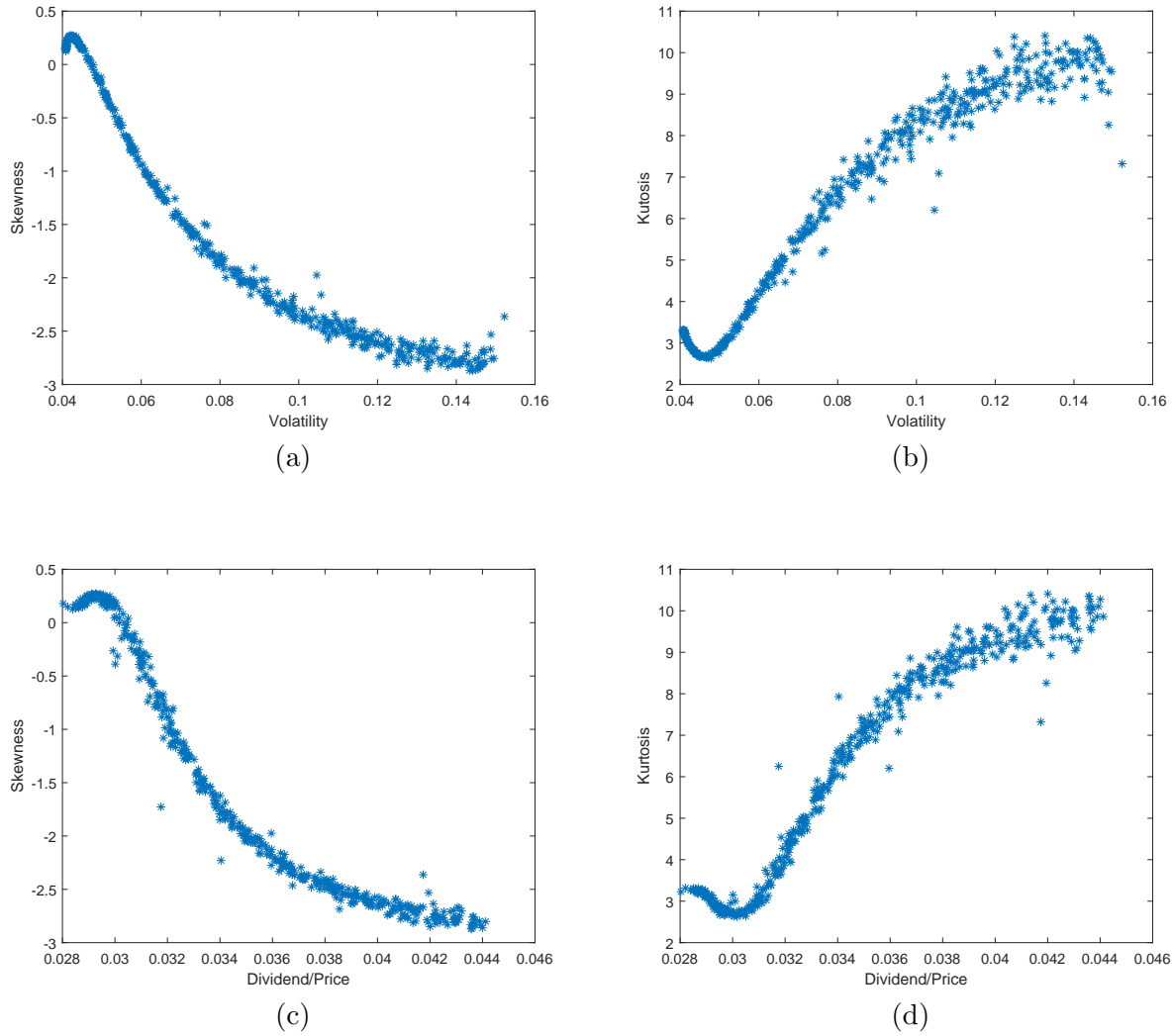
Figure 14: **Higher-moment risk, volatility, and dividend/price ratios in** Gabaix (2012). Panel (a) shows a scatterplot of simulated stock market skewness and volatility. Panel (b) shows a scatterplot of simulated stock market kurtosis and volatility. Panel (c) shows a scatterplot of simulated stock market skewness and the dividend-price ratio. Panel (d) shows a scatterplot of simulated stock market kurtosis and the dividend-price ratio. Simulation details are in Appendix E.2.

Table 1: **Average Implied and Realized Stock Market Moments.** This table reports the average monthly and quarterly horizon values of the *ex ante* risk-neutral and *ex post* realized variance (annualized and in percentages), skewness, and kurtosis of the return distributions for twenty stock market indexes around the world. See Section 2 for a discussion on how we infer the implied and realized moments from options or realized returns.

| | Monthly horizon | | | | | | Quarterly horizon | | | | | | | |
| | Implied moments | | | Realized moments | | | Implied moments | | | Realized moments | | | | |
	var	skew	kurt	var	skew	kurt	var	skew	kurt	var	skew	kurt	Sample start	Sample end
United States														
SP500	4.25	−1.87	21.78	3.63	−2.23	17.70	4.41	−1.45	8.19	3.74	−2.63	15.60	1996-01-31	2020-12-31
NASDAQ	7.76	−1.05	11.27	7.53	−1.47	8.07	7.78	−0.95	5.32	8.01	−1.80	6.92	1996-01-31	2020-12-31
DowJ	4.20	−2.06	31.21	3.43	−1.99	12.15	4.29	−1.50	8.95	3.59	−2.40	13.04	1997-10-31	2020-12-31
Russell	5.90	−1.17	10.11	5.19	−1.64	10.71	5.97	−1.03	5.12	5.47	−1.89	8.36	1996-01-31	2020-12-31
Europe														
BEL	5.47	−1.30	11.34	3.41	−1.57	18.26	5.47	−1.29	6.24	3.41	−2.01	24.30	2002-01-31	2020-12-31
CHE	4.72	−3.02	36.01	2.63	−2.62	29.86	4.62	−2.19	14.14	2.85	−3.18	34.67	2002-01-31	2021-01-29
DEU	6.85	−2.48	27.21	3.41	−3.10	29.68	7.26	−2.14	16.62	3.49	−4.08	41.12	2002-01-31	2021-01-29
ESP	7.68	−1.52	13.93	4.54	−2.05	18.01	7.60	−1.42	7.49	4.72	−2.66	22.53	2007-02-28	2021-01-29
FIN	7.23	−0.82	4.32	6.27	−0.39	3.80	4.71	−0.69	2.90	4.43	−0.57	9.26	2002-02-28	2020-09-30
FRA	6.18	−2.14	16.74	3.41	−3.12	29.32	6.35	−2.10	12.16	3.50	−3.68	36.63	2003-06-30	2021-01-29
GBR	5.60	−3.58	46.91	3.09	−2.79	25.48	5.26	−2.94	25.73	2.98	−3.45	41.80	2002-01-30	2020-12-31
ITA	8.53	−2.19	21.79	4.94	−1.87	20.99	8.83	−2.42	19.95	5.14	−2.53	30.57	2006-11-30	2021-01-29
NLD	6.27	−2.90	37.49	3.21	−3.08	31.79	7.21	−2.11	24.47	3.82	−3.47	32.10	2002-02-28	2021-01-29
SWE	6.17	−2.84	29.39	3.79	−2.22	21.21	6.64	−2.07	12.98	4.24	−2.40	23.23	2007-07-31	2021-01-29
Asia														
AUS	4.40	−2.59	26.96	2.02	−2.85	39.09	4.10	−2.34	17.37	2.22	−2.73	36.09	2007-02-28	2019-12-31
CHN	9.28	−0.97	9.37	6.38	−0.89	15.42	9.98	−1.03	6.69	8.01	−0.97	15.14	2006-03-31	2019-12-31
HKG	7.22	−1.26	11.83	4.64	−1.82	20.50	6.73	−1.29	6.71	4.91	−1.95	18.67	2006-03-31	2019-12-31
JPN	7.25	−2.86	34.84	3.49	−2.43	37.33	6.85	−2.12	18.57	3.91	−2.69	34.37	2004-08-31	2019-12-30
KOR	5.02	−1.34	10.38	2.67	−1.59	8.19	3.78	−0.93	4.29	3.06	−1.26	3.50	2004-08-31	2019-12-30
TWN	4.34	−1.68	8.99	2.13	−1.72	16.00	4.52	−1.36	5.16	2.81	−1.65	10.83	2005-10-31	2019-12-31

Table 2: **Ex ante moments predict ex post realized moments.** The first row of Panel A reports the slope coefficients from panel regressions of the form:

$$\text{Realized moment}^i_{t,T} = \alpha^i + \beta E_t[\text{Moment}^i_{t,T}] + \epsilon^i_{t,T}$$

where i represent the different indexes. We include index fixed effects and cluster standard errors by time and country. The second row of Panel A reports a similar panel regression, but here we standardize the (standardized) moments within each index before pooling them together and running the regression. Panel B reports univariate regressions of realized moments onto expected moments for each individual index. We infer the expected moments from option prices and we use methods described in Neuberger (2012) and Bae and Lee (2021) to infer realized moments (see Section 2). The $t-$statistics in the individual index-wise regressions are corrected for autocorrelation and heteroscedasticity using Newey-West standard errors with 12 lags. We report statistical significance at the 10% level in bold.

| | Month | | | | | | Quarter | | | | | |
| | Skewness | | | Kurtosis | | | Skewness | | | Kurtosis | | |
	β	t-stat.	R^2	β	t-stat.	R^2	β	t-stat.	R^2	β	t-stat.	R^2
Panel A: Pooled panel regressions												
Raw moments	**0.19**	3.01	0.15	**0.16**	1.91	0.05	**0.40**	3.42	0.35	**0.25**	2.51	0.12
Standardized moments	**0.19**	3.20	0.03	**0.14**	4.03	0.01	**0.39**	6.19	0.14	**0.29**	4.42	0.07
Panel B: Index-wise regressions												
United States												
SP500	**0.46**	5.34	0.16	**0.20**	1.91	0.06	**1.02**	5.94	0.40	**1.82**	3.94	0.34
NASDAQ	**0.56**	5.73	0.20	**0.16**	1.71	0.02	**0.88**	8.25	0.43	**1.64**	6.73	0.34
DowJ	**0.18**	2.41	0.05	**0.14**	3.39	0.08	**0.72**	5.49	0.28	**1.26**	2.88	0.15
Russell	**0.42**	5.12	0.07	-0.04	-0.24	0.00	**0.72**	4.59	0.21	**0.98**	2.33	0.03
Europe												
BEL	**0.42**	2.34	0.10	0.12	0.58	0.00	**1.16**	4.39	0.27	1.89	1.35	0.01
CHE	-0.02	-0.25	-0.01	-0.09	-0.80	0.00	**0.72**	3.10	0.16	**1.19**	3.57	0.09
DEU	-0.01	-0.06	0.00	0.08	0.30	0.00	0.95	1.55	0.06	0.50	1.42	-0.01
ESP	-0.13	-0.67	0.00	-0.36	-0.92	0.00	**0.74**	1.69	0.09	**2.66**	2.10	0.13
FIN	-0.02	-0.07	-0.02	-0.96	-1.16	0.00	**0.88**	4.14	0.16	**4.94**	3.67	0.01
FRA	**0.36**	1.95	0.02	0.19	0.91	0.00	0.51	0.90	0.02	0.92	0.84	0.01
GBR	**0.16**	2.51	0.03	-0.03	-0.23	-0.01	0.20	1.26	0.03	0.04	0.16	-0.01
ITA	**0.18**	2.50	0.02	**0.61**	2.57	0.07	**0.26**	2.07	0.09	**0.53**	2.51	0.16
NLD	**0.25**	3.01	0.03	**0.21**	1.78	0.01	**0.18**	5.36	0.09	0.05	1.02	-0.01
SWE	0.08	0.93	0.00	**0.51**	1.67	0.06	**0.29**	2.06	0.04	0.23	1.58	0.00
Asia												
AUS	**0.25**	2.11	0.03	**0.30**	3.17	0.05	**0.20**	2.74	0.02	0.15	1.25	-0.01
CHN	0.51	1.51	0.01	0.09	0.20	-0.01	0.47	1.41	0.02	0.62	1.18	0.01
HKG	0.08	0.37	-0.01	0.14	1.40	0.00	**0.69**	2.45	0.02	0.35	0.28	-0.02
JPN	**0.34**	3.19	0.06	**0.82**	4.97	0.17	**0.61**	3.10	0.13	**0.93**	3.28	0.15
KOR	**0.16**	2.98	0.02	**0.37**	9.19	0.15	**0.71**	4.31	0.11	**2.07**	5.93	0.47
TWN	0.06	0.23	-0.01	**1.06**	1.78	0.03	**1.25**	4.39	0.26	**2.95**	7.14	0.32

Table 3: **Comovements in higher-moment risks.** The first row of Panel A reports the slope coefficients from panel regressions of the form:

$$\text{Skewness}_{t,T}^{i} = \alpha^{i} + \beta \text{Kurtosis}_{t,T}^{i} + \epsilon_{t,T}^{i}$$

where i represent the different indexes. We include index fixed effects and cluster standard errors by time and country. The second row of Panel A reports a similar panel regression, but here we standardize the (standardized) moments within each index before pooling them together and running the regression. Panel B reports univariate regressions of skewness onto kurtosis for each individual index. We infer the expected moments from option prices and we use methods described in Neuberger (2012) and Bae and Lee (2021) to infer realized moments (see Section 2). The $t-$statistics in the individual index-wise regressions are corrected for autocorrelation and heteroscedasticity using Newey-West standard errors with 12 lags. We report statistical significance at the 10% level in bold.

| | Ex ante implied moments | | | | | | Ex post realized moments | | | | | |
| | Monthly | | | Quarterly | | | Monthly | | | Quarterly | | |
	β	t-stat.	R^2	β	t-stat.	R^2	β	t-stat.	R^2	β	t-stat.	R^2
Panel A: Pooled panel regressions												
Raw moments	**−0.04**	−16.24	0.77	−0.01	−0.42	0.26	**−0.02**	−12.85	0.47	**−0.03**	−4.17	0.58
Standardized moments	**−0.75**	−8.97	0.56	**−0.71**	−7.87	0.01	**−0.63**	−21.93	0.39	**−0.72**	−10.57	0.52
Panel B: Index-wise regressions												
United States												
SP500	**−0.03**	−4.69	0.39	**−0.14**	−15.50	0.76	**−0.05**	−12.17	0.56	**−0.07**	−7.43	0.71
NASDAQ	−0.02	−1.48	0.07	**−0.18**	−7.33	0.46	**−0.08**	−7.35	0.51	**−0.11**	−5.38	0.69
DowJ	**−0.03**	−15.28	0.63	**−0.12**	−11.93	0.69	**−0.04**	−5.42	0.26	**−0.04**	−3.21	0.42
Russell	**−0.05**	−5.29	0.25	**−0.13**	−4.84	0.26	−0.02	−1.37	0.10	**−0.05**	−3.35	0.44
Europe												
BEL	**−0.05**	−10.48	0.69	**−0.16**	−4.87	0.50	**−0.02**	−2.32	0.19	**−0.03**	−7.59	0.56
CHE	**−0.04**	−14.73	0.88	**−0.08**	−11.54	0.84	**−0.02**	−8.57	0.45	**−0.03**	−6.14	0.58
DEU	**−0.04**	−18.24	0.88	**−0.05**	−9.55	0.77	**−0.02**	−5.84	0.48	**−0.03**	−16.40	0.89
ESP	**−0.07**	−3.94	0.44	**−0.07**	−2.94	0.24	**−0.02**	−3.89	0.32	**−0.03**	−3.59	0.50
FIN	**−0.15**	−7.36	0.54	**−0.41**	−8.32	0.58	−0.02	−1.14	0.15	**−0.03**	−23.68	0.53
FRA	**−0.05**	−8.85	0.76	**−0.08**	−5.68	0.77	**−0.04**	−15.49	0.66	**−0.03**	−8.49	0.83
GBR	**−0.04**	−28.14	0.94	**−0.05**	−23.09	0.94	**−0.02**	−7.37	0.54	**−0.02**	−2.26	0.31
ITA	**−0.07**	−22.72	0.87	**−0.06**	−22.97	0.94	**−0.02**	−8.99	0.45	**−0.02**	−2.56	0.37
NLD	**−0.04**	−17.30	0.82	**0.05**	6.32	0.65	**−0.02**	−3.04	0.39	**−0.04**	−7.63	0.64
SWE	**−0.06**	−33.88	0.94	**−0.06**	−10.50	0.86	**−0.02**	−5.88	0.53	**−0.04**	−7.95	0.71
Asia												
AUS	**−0.03**	−6.59	0.65	**−0.05**	−17.60	0.90	**−0.02**	−3.60	0.25	0.01	0.72	0.04
CHN	**−0.05**	−6.85	0.41	**−0.06**	−8.37	0.52	**−0.04**	−7.29	0.46	**−0.05**	−10.04	0.67
HKG	**−0.04**	−12.18	0.57	**−0.08**	−3.04	0.26	**−0.05**	−4.82	0.55	**−0.08**	−7.64	0.76
JPN	**−0.06**	−15.17	0.89	**−0.07**	−11.20	0.87	**−0.03**	−9.14	0.54	**−0.05**	−7.43	0.70
KOR	**−0.07**	−16.22	0.79	**−0.12**	−12.21	0.71	**−0.05**	−6.79	0.40	**−0.05**	−4.94	0.30
TWN	**−0.10**	−8.52	0.66	**−0.20**	−4.40	0.62	**−0.04**	−6.65	0.45	**−0.11**	−18.69	0.78

43

Table 4: **Tail-risk is high when variance is low — Ex ante implied moments.** The first row of Panel A reports the slope coefficients from panel regressions of the form:

$$E_t[\text{Moment}_{t,T}^i] = \alpha^i + \beta E_t[\text{Variance}_{t,T}^i] + \epsilon_{t,T}^i$$

where i represent the different indexes. Variances are annualized and in percentages. We include index fixed effects and cluster standard errors by time and country. The second row of Panel A reports a similar panel regression, but here we standardize the (standardized) moments within each index before pooling them together and running the regression. Panel B reports univariate regressions of expected moments onto expected variance for each individual index. We infer the expected moments from option prices (see Section 2). The $t-$statistics in the individual index-wise regressions are corrected for autocorrelation and heteroscedasticity using Newey-West standard errors with 12 lags. We report statistical significance at the 10% level in bold.

	Monthly horizon						Quarterly horizon					
	Skewness			Kurtosis			Skewness			Kurtosis		
	β	t-stat.	R^2	β	t-stat.	R^2	β	t-stat.	R^2	β	t-stat.	R^2
Panel A: Pooled panel regressions												
Raw moments	**0.08**	7.31	0.30	**−1.19**	−6.61	0.17	**0.05**	4.08	0.28	**−0.51**	−3.22	0.19
Standardized moments	**0.37**	6.80	0.13	**−0.28**	−8.12	0.07	**0.33**	4.86	0.10	**−0.29**	−5.39	0.08
Panel B: Index-wise regressions												
United States												
SP500	**0.13**	3.82	0.22	**−2.14**	−3.29	0.14	**0.12**	4.83	0.31	**−0.72**	−3.84	0.31
NASDAQ	**0.07**	6.99	0.51	**−0.25**	−2.05	0.05	**0.07**	9.11	0.62	**−0.17**	−2.95	0.26
DowJ	**0.20**	4.42	0.30	**−3.10**	−3.15	0.13	**0.16**	4.91	0.52	**−0.93**	−4.37	0.35
Russell	**0.07**	5.44	0.20	−0.20	−0.98	0.01	**0.06**	4.71	0.20	−0.12	−1.07	0.04
Europe												
BEL	**0.03**	2.78	0.02	**−0.38**	−2.38	0.01	**0.05**	3.53	0.12	−0.12	−1.77	0.03
CHE	**0.12**	4.84	0.07	**−2.59**	−4.46	0.06	**0.08**	3.34	0.17	**−0.95**	−4.86	0.19
DEU	**0.07**	7.14	0.16	**−1.38**	−5.93	0.13	**0.04**	3.58	0.18	**−0.74**	−4.94	0.20
ESP	**0.05**	2.32	0.03	**−0.71**	−3.55	0.06	**0.04**	3.04	0.08	**−0.26**	−5.60	0.09
FIN	0.02	1.31	0.02	**−0.10**	−1.84	0.02	0.05	1.28	0.04	−0.07	−0.71	0.01
FRA	**0.06**	3.91	0.09	**−0.97**	−4.47	0.11	**0.04**	2.62	0.07	**−0.57**	−3.02	0.11
GBR	**0.18**	4.24	0.16	**−3.77**	−3.51	0.12	**0.15**	4.06	0.19	**−2.23**	−2.98	0.13
ITA	**0.08**	5.15	0.08	**−1.21**	−6.59	0.09	**0.08**	2.69	0.06	**−1.18**	−2.30	0.06
NLD	**0.10**	6.20	0.15	**−2.26**	−4.77	0.12	0.03	0.80	−0.01	**−1.64**	−2.68	0.05
SWE	**0.10**	4.28	0.07	**−1.60**	−3.60	0.08	**0.05**	3.11	0.04	**−0.71**	−2.33	0.02
Asia												
AUS	**0.07**	2.77	0.03	**−1.15**	−1.85	0.01	**0.08**	3.00	0.03	−0.80	−1.43	0.00
CHN	**0.02**	3.57	0.05	**−0.38**	−3.81	0.09	0.01	0.92	0.00	**−0.16**	−2.17	0.06
HKG	**0.04**	6.01	0.07	**−0.77**	−4.01	0.07	**0.01**	1.72	0.01	**−0.17**	−5.75	0.23
JPN	**0.06**	2.24	0.06	**−1.35**	−2.44	0.10	0.01	0.17	−0.02	−0.67	−1.22	0.02
KOR	**0.03**	2.76	0.03	**−0.45**	−2.24	0.03	**0.06**	2.73	0.14	**−0.41**	−1.84	0.12
TWN	**0.07**	4.19	0.20	**−0.61**	−3.47	0.24	**0.10**	4.75	0.28	**−0.44**	−3.68	0.38

Table 5: **Tail-risk is high when variance is low — Ex post realized moments.** The first row of Panel A reports the slope coefficients from panel regressions of the form:

$$\text{Realized moment}_{t,T}^i = \alpha^i + \beta \text{Realized variance}_{t,T}^i + \epsilon_{t,T}^i$$

where i represent the different indexes. Variances are annualized and in percentages. We include index fixed effects and cluster standard errors by time and country. The second row of Panel A reports a similar panel regression, but here we standardize the (standardized) moments within each index before pooling them together and running the regression. Panel B reports univariate regressions of realized moments onto the realized variance for each individual index. We use methods described in Neuberger (2012) and Bae and Lee (2021) to infer realized moments (see Section 2). The $t-$statistics in the individual index-wise regressions are corrected for autocorrelation and heteroscedasticity using Newey-West standard errors with 12 lags. We report statistical significance at the 10% level in bold.

| | Monthly horizon | | | | | | Quarterly horizon | | | | | |
| | Skewness | | | Kurtosis | | | Skewness | | | Kurtosis | | |
	β	t-stat.	R^2	β	t-stat.	R^2	β	t-stat.	R^2	β	t-stat.	R^2
Panel A: Pooled panel regressions												
Raw moments	**0.03**	5.73	0.15	**−0.62**	−3.12	0.17	**0.05**	5.66	0.32	**−0.97**	−3.47	0.14
Standardized moments	**0.14**	4.07	0.01	**−0.16**	−4.13	0.02	**0.25**	4.47	0.05	**−0.25**	−5.05	0.05
Panel B: Index-wise regressions												
United States												
SP500	**0.02**	3.21	0.02	**−0.53**	−2.76	0.05	**0.06**	2.94	0.07	**−0.75**	−2.54	0.10
NASDAQ	**0.02**	4.77	0.08	**−0.23**	−4.46	0.10	**0.04**	6.06	0.28	**−0.28**	−3.54	0.20
DowJ	**0.02**	3.52	0.02	**−0.29**	−2.25	0.02	**0.06**	3.61	0.10	**−0.76**	−2.33	0.06
Russell	**0.02**	2.36	0.02	**−0.29**	−1.94	0.02	**0.03**	2.24	0.05	**−0.31**	−1.72	0.03
Europe												
BEL	**0.04**	2.63	0.02	**−0.73**	−2.26	0.01	0.07	1.47	0.01	−1.70	−1.62	0.02
CHE	0.04	1.34	0.00	**−1.69**	−2.05	0.01	**0.09**	2.40	0.08	**−2.64**	−4.39	0.10
DEU	**0.05**	3.51	0.02	**−0.99**	−1.74	0.00	**0.08**	2.46	0.02	**−1.93**	−1.73	0.01
ESP	0.03	1.51	0.00	**−0.71**	−1.66	0.00	**0.07**	3.82	0.06	**−1.53**	−4.09	0.06
FIN	**0.05**	2.90	0.06	−0.18	−0.41	−0.02	**0.13**	3.44	0.16	−1.28	−1.45	0.01
FRA	**0.06**	3.50	0.04	**−1.26**	−2.79	0.03	**0.08**	3.98	0.04	**−1.91**	−2.76	0.02
GBR	**0.04**	2.54	0.01	−0.75	−1.23	0.00	**0.08**	3.78	0.04	**−3.18**	−4.10	0.06
ITA	**0.03**	2.35	0.01	**−0.90**	−2.31	0.01	**0.07**	4.50	0.11	**−1.93**	−4.22	0.09
NLD	**0.07**	2.95	0.03	**−1.71**	−2.80	0.01	**0.08**	2.36	0.07	**−1.53**	−2.60	0.05
SWE	**0.04**	3.20	0.02	**−1.25**	−2.27	0.00	**0.09**	3.37	0.09	**−1.46**	−2.41	0.05
Asia												
AUS	0.05	1.30	0.00	**−4.48**	−3.06	0.05	−0.04	−1.32	−0.01	**−2.72**	−1.93	0.00
CHN	0.01	0.87	−0.01	**−0.57**	−2.52	0.01	0.01	0.53	−0.02	**−0.45**	−2.24	0.02
HKG	0.01	0.59	−0.01	**−0.43**	−2.61	0.01	0.02	0.90	−0.01	**−0.47**	−2.60	0.03
JPN	0.02	0.79	−0.01	**−2.05**	−2.24	0.03	0.01	0.56	−0.01	**−1.37**	−2.18	0.03
KOR	0.01	0.73	−0.01	−0.63	−1.59	0.01	**0.08**	5.92	0.09	−0.41	−1.29	0.01
TWN	−0.05	−0.58	−0.01	−1.70	−1.58	0.01	**0.16**	2.81	0.09	**−1.45**	−4.84	0.10

Table 6: **Cyclicality in higher-moment risks — Divided-Price Ratio (Ex ante implied moments).** The first row of Panel A reports the slope coefficients from panel regressions of the form:

$$E_t[\text{Moment}^i_{t,T}] = \alpha^i + \beta\text{Dividend-Price Ratio}^i_t + \gamma t + \epsilon^i_{t,T}$$

where i represent the different indexes and Dividend-Price Ratio^i_t dividend-price ratio at time t for index i. We include index fixed effects and cluster standard errors by time and country. The second row of Panel A reports a similar panel regression, but here we standardize the (standardized) moments and the past returns within each index before pooling them together and running the regression. Panel B reports univariate regressions of realized moments onto the past returns for each individual index. We use methods described in Neuberger (2012) and Bae and Lee (2021) to infer realized moments (see Section 2). The $t-$statistics in the individual index-wise regressions are corrected for autocorrelation and heteroscedasticity using Newey-West standard errors with 12 lags. We report statistical significance at the 10% level in bold.

	Monthly horizon						Quarterly horizon					
	Skewness			Kurtosis			Skewness			Kurtosis		
	β	t-stat.	R^2	β	t-stat.	R^2	β	t-stat.	R^2	β	t-stat.	R^2
Panel A: Pooled panel regressions												
Raw moments	7.16	1.53	0.00	−100.75	−1.28	0.00	**1.85**	2.46	−0.00	−20.05	−1.00	−0.00
Standardized moments	**0.17**	4.78	0.02	**−0.10**	−2.96	0.01	**0.14**	2.33	0.01	**−0.12**	−2.64	0.00
Panel B: Index-wise regressions												
United States												
SP500	45.09	1.56	0.23	**−912.49**	−2.25	0.04	49.95	1.54	0.41	**−261.26**	−2.49	0.38
NASDAQ	5.07	0.22	0.28	−120.26	−0.49	0.00	5.74	0.30	0.35	−42.57	−0.89	0.46
DowJ	**108.67**	4.17	0.24	−279.83	−0.44	0.10	**51.38**	2.77	0.39	**−237.56**	−1.71	0.21
Russell	**45.78**	2.14	0.16	213.76	1.64	0.13	**43.43**	2.36	0.12	38.18	0.72	0.35
Europe												
BEL	−2.13	−0.51	0.02	−68.90	−1.28	0.00	−3.74	−1.17	−0.01	**18.73**	1.86	−0.01
CHE	**57.81**	4.13	0.10	**−1210.43**	−2.79	0.04	**16.08**	3.26	0.54	**−175.36**	−2.26	0.40
DEU	**26.68**	3.48	0.08	**−598.61**	−3.16	0.06	**7.07**	1.77	0.26	**−166.44**	−2.73	0.09
ESP	16.46	1.50	0.01	**−225.61**	−2.42	0.10	**15.99**	3.78	0.13	**−76.51**	−3.90	0.04
FIN	**2.02**	3.47	0.11	**−6.04**	−1.92	0.00	**2.07**	4.90	0.07	**−3.41**	−3.82	0.13
FRA	**33.44**	3.93	0.24	**−494.24**	−3.05	0.13	**30.19**	6.64	0.28	**−277.08**	−4.51	0.17
GBR	**74.43**	4.17	0.38	**−1259.79**	−3.14	0.36	**46.43**	6.92	0.26	**−593.54**	−3.55	0.20
ITA	**39.14**	2.89	0.08	**−516.65**	−2.88	0.08	**29.33**	2.32	0.21	**−324.07**	−1.66	0.16
NLD	**22.47**	2.76	0.12	**−502.41**	−2.71	0.06	−20.86	−1.15	0.13	**−519.17**	−1.95	0.00
SWE	**20.57**	1.93	0.07	−264.98	−1.46	0.04	**17.87**	2.86	0.11	**−190.20**	−2.41	0.04
Asia												
AUS	23.96	1.26	0.02	−279.36	−0.71	−0.01	10.08	0.55	0.02	31.98	0.10	−0.02
HKG	**8.82**	1.76	0.05	**−141.48**	−2.06	0.02	6.46	1.63	0.03	**−63.79**	−2.97	0.13
JPN	−25.75	−1.23	0.64	435.42	0.95	0.55	**−48.03**	−2.25	0.63	118.54	0.46	0.45

46

Table 7: **Cyclicality in higher-moment risks — Divided-Price Ratio (Ex post realized moments).** The first row of Panel A reports the slope coefficients from panel regressions of the form:

$$\text{Realized moment}^i_{t,T} = \alpha^i + \beta \text{Dividend-Price Ratio}^i_t + \gamma t + \epsilon^i_{t,T}$$

where i represent the different indexes and Dividend-Price Ratio^i_t dividend-price ratio at time t for index i. We include index fixed effects and cluster standard errors by time and country. The second row of Panel A reports a similar panel regression, but here we standardize the (standardized) moments and the past returns within each index before pooling them together and running the regression. Panel B reports univariate regressions of realized moments onto the past returns for each individual index. We use methods described in Neuberger (2012) and Bae and Lee (2021) to infer realized moments (see Section 2). The $t-$statistics in the individual index-wise regressions are corrected for autocorrelation and heteroscedasticity using Newey-West standard errors with 12 lags. We report statistical significance at the 10% level in bold.

| | Monthly horizon | | | | | | Quarterly horizon | | | | | |
| | Skewness | | | Kurtosis | | | Skewness | | | Kurtosis | | |
	β	t-stat.	R^2	β	t-stat.	R^2	β	t-stat.	R^2	β	t-stat.	R^2
Panel A: Pooled panel regressions												
Raw moments	3.11	1.18	0.13	−25.53	−0.59	0.04	**3.65**	2.84	0.26	**−93.51**	−1.95	0.10
Standardized moments	0.04	1.07	0.00	−0.02	−0.84	0.00	**0.05**	1.03	−0.00	**−0.10**	−2.39	−0.00
Panel B: Index-wise regressions												
United States												
SP500	18.09	0.83	0.09	**−560.07**	−1.69	0.10	22.12	0.72	0.31	**−555.27**	−1.96	0.28
NASDAQ	−9.23	−0.66	0.19	−112.79	−1.13	0.20	−17.97	−1.00	0.45	−62.60	−0.45	0.47
DowJ	3.79	0.19	0.02	−102.14	−0.53	0.03	7.04	0.33	0.20	−393.02	−1.46	0.17
Russell	−18.28	−0.53	0.00	432.15	0.66	0.04	−21.62	−0.46	−0.01	588.44	0.71	0.02
Europe												
BEL	−10.53	−1.36	0.12	**262.62**	2.04	0.05	−14.41	−1.53	0.16	7.59	0.05	0.01
CHE	−0.87	−0.08	0.08	238.80	0.55	0.01	**26.85**	2.39	0.21	**−1055.26**	−2.76	0.11
DEU	17.29	1.35	0.04	106.76	0.30	0.02	42.04	1.35	0.20	−1124.12	−1.09	0.15
ESP	**21.19**	2.59	0.02	−316.74	−1.14	−0.01	**31.69**	3.43	0.07	**−685.23**	−3.57	0.07
FIN	1.01	1.60	−0.02	−8.73	−0.62	−0.04	**3.26**	2.83	0.05	**−49.74**	−2.12	0.02
FRA	**38.45**	3.04	0.02	**−669.13**	−2.97	0.01	**55.70**	3.50	0.11	**−1082.95**	−2.62	0.08
GBR	18.72	1.59	0.00	−220.72	−0.89	−0.01	**22.96**	1.71	0.13	**−1064.80**	−3.37	0.07
ITA	−1.91	−0.17	−0.01	278.23	0.85	−0.01	**26.63**	3.08	0.16	**−898.54**	−3.25	0.07
NLD	**25.09**	4.48	0.02	**−590.87**	−2.74	0.00	1.85	0.18	0.11	−265.14	−1.37	0.00
SWE	**21.40**	1.69	0.08	−233.56	−1.14	0.02	**42.33**	1.80	0.35	**−799.15**	−1.72	0.14
Asia												
AUS	**29.81**	2.29	0.02	−646.49	−1.33	0.00	−20.42	−1.22	−0.02	−724.68	−1.35	−0.02
HKG	5.22	0.21	−0.01	−96.88	−0.38	−0.01	3.63	0.17	−0.02	−250.36	−1.26	0.01
JPN	−14.81	−0.30	0.05	311.70	0.55	0.11	**−169.92**	−3.65	0.24	**2071.92**	3.06	0.26

Table 8: **Cyclicality in higher-moment risks — Alternative indicators of the state of the economy.** This table reports the slope coefficients from index-wise regressions on the form:

$$\text{Moment}_{t,T} = \alpha + \beta \text{Indicator}_t + \gamma t + \epsilon_{t,T}$$

where Indicator_t is: (Panel A) the consumption-wealth ratio of Lettau and Ludvigson (2001) scaled by 100 for readability, (Panel B) the Chicago Fed National Activity Index, and (Panel C) NBER recession periods. $\text{Moment}_{t,T}$ is either the expected moments or the realized moments. We infer the expected moments from option prices and we use methods described in Neuberger (2012) and Bae and Lee (2021) to infer realized moments (see Section 2). The $t-$statistics are corrected for autocorrelation and heteroscedasticity using Newey-West standard errors with 12 lags. We report statistical significance at the 10% level in bold.

| | Monthly horizon | | | | | | Quarterly horizon | | | | | |
| | Skewness | | | Kurtosis | | | Skewness | | | Kurtosis | | |
	β	t-stat.	R^2	β	t-stat.	R^2	β	t-stat.	R^2	β	t-stat.	R^2
Panel A: Consumption-wealth ratio ('cay' from Lettau and Ludvigson (2001))												
Implied moments												
SP500	**0.26**	2.07	0.26	**−4.84**	−1.88	0.05	**0.13**	1.92	0.40	**−0.76**	−1.83	0.41
NASDAQ	0.09	1.03	0.33	−0.26	−0.18	0.01	**0.16**	1.88	0.41	−0.11	−0.42	0.55
DowJ	0.30	1.45	0.25	−5.06	−1.16	0.16	**0.17**	1.67	0.51	**−1.21**	−1.97	0.35
Russell	**0.23**	2.39	0.17	−0.93	−1.10	0.16	**0.24**	2.61	0.14	**−0.50**	−2.11	0.41
Realized moments												
SP500	**0.20**	1.72	0.10	**−4.27**	−2.30	0.11	**0.19**	1.74	0.36	**−2.55**	−1.75	0.31
NASDAQ	**0.11**	1.65	0.22	**−1.10**	−1.70	0.22	0.09	1.27	0.49	−0.33	−0.55	0.52
DowJ	0.16	1.27	0.03	−1.92	−1.17	0.04	**0.17**	1.68	0.27	−0.92	−0.63	0.22
Russell	0.09	0.81	0.00	1.19	0.49	0.04	0.15	1.31	0.00	0.44	0.27	−0.01
Panel B: Chicago Fed National Activity Index (CFNAI)												
Implied moments												
SP500	**−0.51**	−3.58	0.06	**7.32**	3.08	0.03	**−0.47**	−4.15	0.14	**2.19**	3.27	0.08
NASDAQ	**−0.24**	−2.01	0.02	−0.14	−0.10	0.00	**−0.29**	−2.76	0.06	0.47	1.19	0.00
DowJ	**−0.75**	−4.25	0.07	**8.38**	2.13	0.01	**−0.45**	−4.77	0.13	**2.67**	3.53	0.09
Russell	**−0.38**	−3.36	0.07	−0.74	−0.67	0.00	**−0.41**	−6.34	0.13	0.28	0.67	−0.01
Realized moments												
SP500	−0.19	−1.36	0.00	**6.32**	3.52	0.03	−0.30	−1.63	0.01	**4.86**	2.05	0.03
NASDAQ	−0.02	−0.18	0.00	0.69	0.67	0.00	−0.13	−1.11	0.00	**1.65**	1.81	0.01
DowJ	**−0.23**	−2.17	0.01	**2.75**	1.68	0.00	**−0.27**	−2.35	0.01	**4.70**	2.17	0.02
Russell	**−0.36**	−2.86	0.02	**7.02**	1.81	0.04	**−0.43**	−2.45	0.05	4.96	1.62	0.04
Panel C: NBER recessions												
Implied moments												
SP500	**0.88**	3.19	0.08	**−12.48**	−4.07	0.04	**0.83**	2.89	0.18	**−3.82**	−2.89	0.10
NASDAQ	**0.63**	2.76	0.08	**−3.33**	−1.75	0.01	**0.49**	2.29	0.08	**−1.28**	−1.83	0.03
DowJ	**1.46**	5.08	0.13	**−19.37**	−3.65	0.04	**0.82**	4.48	0.18	**−4.84**	−3.73	0.12
Russell	**0.65**	4.23	0.09	−2.51	−1.39	0.01	**0.51**	3.13	0.08	−1.00	−1.49	0.01
Realized moments												
SP500	0.29	1.20	0.00	−6.88	−1.63	0.01	**0.57**	1.97	0.03	**−8.32**	−2.29	0.04
NASDAQ	0.21	1.34	0.00	−2.58	−1.62	0.01	0.30	1.35	0.01	**−3.26**	−1.81	0.02
DowJ	**0.42**	2.77	0.01	**−5.95**	−3.23	0.02	**0.54**	2.60	0.03	**−8.61**	−2.48	0.03
Russell	**0.48**	2.95	0.02	**−5.37**	−2.01	0.01	**0.60**	2.97	0.05	**−5.32**	−2.03	0.01

48

Table 9: **The common tail-risk component in international stock markets.** The first column of Panel A reports: (i) the coefficients of the first principal component of the space spanned by monthly horizon ex ante variance for the twenty stock market indexes and (ii) the percentage of the variation explained by the first principal component. The second column reports the slope coefficient of index-wise regressions of the form:

$$\text{Variance}^i_{t,T} = \alpha^i + \beta^i \text{Variance PC1}_{t,T} + \epsilon^i_{t,T}$$

Where Variance $\text{PC1}_{t,T}$ is the first principal component of variances for the twenty indexes. The third column reports $t-$statistics that we correct for autocorrelation and heteroscedasticity using Newey-West standard errors with 12 lags. The fourth column reports the adjusted R^2. Columns five to twelve report the results of a similar analysis for ex ante skewness and ex ante kurtosis. Panel B reports the slope, $t-$statistics, and adjusted R^2 of the regression: Skew $\text{PC1}_{t,T} = \alpha + \beta \text{Var PC1}_{t,T} + \epsilon_{t,T}$ and similarly for kurtosis instead of skewness. Significance at the 10% level is shown in bold.

Panel A: First principal component and index-wise regressions

	Ex ante log(variance)				Ex ante skewness				Ex ante kurtosis			
	Var PC1	β	t-stat.	R^2	Skew PC1	β	t-stat.	R^2	Kurt PC1	β	t-stat.	R^2
United States												
SP500	0.24	**0.17**	31.98	0.92	0.28	**2.36**	10.32	0.64	0.21	**3.31**	5.26	0.39
NASDAQ	0.22	**0.14**	16.57	0.83	0.20	**3.09**	3.87	0.32	0.07	**0.59**	1.99	0.03
DowJ	0.23	**0.15**	22.57	0.89	0.27	**1.55**	8.07	0.58	0.24	**8.43**	6.48	0.49
Russell	0.23	**0.15**	30.60	0.90	0.25	**3.18**	7.11	0.49	0.14	**1.32**	4.06	0.17
Europe												
BEL	0.22	**0.14**	14.61	0.79	0.05	0.57	0.97	0.01	0.19	**1.67**	4.73	0.29
CHE	0.23	**0.14**	26.63	0.90	0.27	**1.26**	7.31	0.61	0.29	**11.51**	10.01	0.70
DEU	0.23	**0.14**	21.73	0.89	0.28	**2.03**	9.56	0.65	0.30	**7.01**	13.35	0.75
ESP	0.21	**0.13**	12.28	0.72	0.08	0.42	1.56	0.04	0.21	**3.27**	3.51	0.36
FIN	0.20	**0.13**	14.81	0.68	0.14	**1.89**	2.70	0.15	0.09	**0.23**	2.77	0.07
FRA	0.23	**0.15**	17.12	0.89	0.28	**2.97**	8.85	0.65	0.29	**3.66**	9.38	0.73
GBR	0.24	**0.15**	47.02	0.94	0.26	**0.95**	6.41	0.55	0.24	**12.45**	7.64	0.48
ITA	0.18	**0.10**	8.84	0.53	0.24	**1.32**	7.42	0.47	0.26	**5.32**	9.60	0.60
NLD	0.24	**0.16**	30.25	0.93	0.29	**1.70**	10.64	0.71	0.29	**9.81**	18.22	0.71
SWE	0.24	**0.15**	42.39	0.91	0.25	**1.05**	7.67	0.51	0.27	**8.03**	9.43	0.61
Asia												
AUS	0.23	**0.16**	21.45	0.89	0.13	**0.67**	2.48	0.14	0.10	**4.14**	1.71	0.08
CHN	0.22	**0.15**	15.18	0.78	0.15	**1.43**	4.74	0.18	0.20	**2.45**	10.28	0.33
HKG	0.22	**0.16**	14.40	0.79	0.16	**1.08**	4.01	0.19	0.18	**4.08**	3.70	0.28
JPN	0.20	**0.12**	9.38	0.66	0.23	**1.29**	5.18	0.44	0.22	**5.85**	5.62	0.40
KOR	0.22	**0.16**	16.34	0.81	0.18	**1.50**	4.72	0.25	0.22	**2.74**	2.83	0.41
TWN	0.22	**0.17**	24.57	0.82	0.25	**2.90**	7.58	0.51	0.28	**1.62**	11.14	0.65
Variation explained	83%				41%				43%			

Panel B: Higher-moment PC1 regressed onto variance PC1

	β	t-stat.	R^2
Skew PC1	**0.54**	10.40	0.59
Kurt PC1	**−0.69**	−6.28	0.42

Table 10: **Higher-moment risk and risk premia in theory and in the data.** This table reports the results of regressions of ex post realized returns onto the ex ante skewness. The first two columns shows results on simulated data from the Wachter (2013). We estimate expected skewness by projecting realized daily skewness for the upcoming month onto the ex ante disaster intensity. We then regress ex post realized returns of a given month based on the (normalized) ex ante skewness in 40,000 samples of 30-year length each and report median slope coefficients. Standard errors are obtained as the standard deviation of the simulated parameters. We refer to Appendix E.1 for details on this procedure. In column 3-6, we project realized monthly returns on ex ante risk-neutral skewness in our panel of 17 countries. We include country fixed effects and double cluster standard errors by country and date. We normalize skewness by dividing by the standard deviation of the skewness in the given country. Returns are in percent. The sample includes the 17 countries listed in Table 1. Standard errors are reported in parentheses below the parameters and statistical significance at the 5-percent level is reported in bold.

	Wachter (2013)		Regression results in global panel			
	Ex. ret	Raw ret	Ex. ret	Raw ret	Ex. ret	Raw ret
Skewness (normalized)	−0.75 (0.85)	−0.73 (0.96)	−0.20 (0.23)	−0.27 (0.18)	−0.30 (0.18)	**−0.31** (0.14)
Variance (normalized)					0.32 (0.53)	0.12 (0.38)
R^2	0.012	0.012	0.003	0.005	0.005	0.005
N	300	300	3,380	3,398	3,380	3,398
FE	NA	NA	Country	Country	Country	Country

Appendix

Appendix A Alternative choices for excluding/including data in the estimation of implied moments

In the following, we describe four alternative ways in which we have excluded/included option data to fit implied moments. Tables A5 to A9 in the online appendix, report the robustness results of our analysis in Tables 2, 3, 4, and 6 where we use the alternative methods to estimate moments. Overall, we find that our results are robust to the alternative choices of excluding/including option data into our analysis.

Detrended moments using all observable prices. As a first robustness test of our results, we rerun our analysis using detrended moments. That is, we first estimate moments using all observable option prices and thereafter we linearly detrend the moments using calendar dates as our detrending variable. The detrending is meant to capture the effect that the moments are mechanically increasing over time in our sample due to the increasing number of options traded at different strikes. Panel A of Tables A5 to A9 in the online appendix report the results of the panel regressions in Tables 2, 3, 4, and 6 using the detrended implied moments.

Dynamic bounds with extrapolation. Let $\sigma_{t,T}$ be the time t risk-neutral volatility of market returns. In this method, we first use *all* available option prices for a given index to estimate a time-series of $\sigma_{t,T}$ using the methods described in Section 2.1. Thereafter, on each date, we select the observed options that are within the range from spot$-5\sigma_{t,T}$ to spot$+5\sigma_{t,T}$. If on a given date there are no options traded with strikes as far as $\pm 5\sigma_{t,T}$ from the spot price then we extrapolate prices using a nearest neighbor methodology on implied volatilities. In the end, we end up with a homogeneous dataset meant in the sense that we have option data that span the same number of conditional risk-neutral volatilities on each date. Panel B of Tables A5 to A9 in the online appendix report the results of the panel regressions in Tables 2, 3, 4, and 6 using the dynamic bounds to estimate implied moments.

Static bounds without extrapolation. In this method, we use the observable options with strikes in the range from spot$\times 0.65$ to spot$\times 1.35$. All observations outside this range are excluded and we do not extrapolate to obtain prices for the entire range if these are not

in the data. Panel C of Tables A5 to A9 in the online appendix report the results of the panel regressions in Tables 2, 3, 4, and 6 using the static bounds without extrapolation to estimate implied moments.

Static bounds with extrapolation. Lastly, we consider use the observable options with strikes in the range from spot×0.75 to spot×1.25 for monthly horizon and the range from spot×0.55 to spot×1.45 for the quarterly horizon. All observations outside this range are excluded. We use a nearest neighbor extrapolation method to extrapolate data to cover the entire range if these are not in the data. Panel D of Tables A5 to A9 in the online appendix report the results of the panel regressions in Tables 2, 3, 4, and 6 using the static bounds with extrapolation to estimate implied moments.

Appendix B   Comments on the estimation of Tail Probabilities

To estimate the first derivative of the put option price written on the risky asset at strike $\alpha S_t - D_{t,T}$ and to handle a sparse and discrete set of observed option prices, we smoothen observed option prices using a polynomial prediction of observed implied volatilities (IV) onto their option strikes. Specifically, in the spirit of Dumas, Fleming, and Whaley (1998), we regress observed implied volatilities onto their respective strikes:

$$IV_i = \beta_0 + \beta_1 \text{Strike}_i + \beta_2 \text{Strike}_i^2 + \beta_3 \text{Strike}_i^3 + \eta_i \tag{26}$$

It is important to note that we run this regression on the put side of the implied volatility surface only. That is, we use observations from the put with the lowest observable strike to the put with the strike that is closest to the forward price but still lower than the forward price. We disregard the call side of the implied volatility surface because we do not need this part in our estimation of left-tail probabilities. The fact that we only have to smoothen the put side of the implied volatility surface is a huge advantage simply because we only have to fit the left side of the well-known implied volatility smirk. It is a lot easier to fit one side of the surface accurately than the entire surface because most of the non-linearity in the surface arises around the forward price.

We also note that we fit a third degree polynomial to the put-side of the implied volatility surface only when we have more than 50 put options with different strikes. If we have between

10 and 49, we fit a second degree polynomial and if we have less than 10 put options with different strikes for a given day and horizon, we use a first order polynomial. The cut-off points for when we use the different polynomials is quite ad-hoc and choosing other thresholds has little importance for our results. The important thing is that we do not overfit the surface when we have only a few observations. Figure A2 in the online Appendix shows examples of fitted implied put volatilities and the option prices.

Now, given a smooth set of option prices around the strike $\alpha S_t - D_{t,T}$, we compute the first derivative as the slope between the two adjacent prices:

$$\text{put}'_{t,T}(\alpha S_t - D_{t,T}) = \frac{\text{put}_{t,T}(\alpha S_t - D_{t,T} + h) - \text{put}_{t,T}(\alpha S_t - D_{t,T} - h)}{2h} \tag{27}$$

where h is the chosen grid step size in the discretization.

Appendix C   Computing Bollerslev, Todorov, and Xu (2015) parameters

According to Bollerslev, Todorov, and Xu (2015), the left tail parameters can be computed from out-of-the-money put options in the following way:

$$\alpha_t^- = \text{median}_{2 \leq i \leq N} \left| 1 - \frac{\ln \frac{O_{t,T}(k_{i,t})}{O_{t,T}(k_{i-1,t})}}{k_{i,t} - k_{i-1,t}} \right| \tag{28}$$

and

$$\phi_t^- = \text{median}_{2 \leq i \leq N} \left| \ln \frac{e^{r_{t,T}} O_{t,T}(k_{i,t})}{(T-t) F_{t,T}} - (1 + \alpha_t^-) k_{i,t} + \ln(\alpha_t^- + 1) + \ln(\alpha_t^-) \right| \tag{29}$$

where N is the number of available options, $O_{t,T}(k_{i,t})$ is the mid-price of the i'th option ordered according to the log-moneyness, $k_{i,t}$, and $r_{t,T}$ is the risk-free interest rate. Code and detailed empirical description can be found on the Torben Andersen and Viktor Todorov derivatives-based market indicators website: tailindex.com. We follow the description outlined on the website step-by-step.

Appendix D Skewness in jump diffusion Models

In this section, we discuss the skewness of various jump diffusion models. Our analysis springs from the results of Zhen and Zhang (2020), who derives the theoretical skewness in a five-factor jump diffusion model with stochastic variance and jump intensity, correlated variance and returns, and jumps in prices and variances. We investigate a particular version of their model, where returns are given as:

$$\frac{dS_t}{S_t} = \alpha dt + \sigma_t dB_t^S + (e^x - 1)dN_t - \lambda_t E(e^x - 1)dt \tag{30}$$

$$d\sigma_t^2 = k_\sigma(\bar{\sigma}^2 - \sigma_t^2)dt + \sigma_\sigma\sqrt{\sigma_t^2}dB_t^\sigma + ydN_t - \lambda_t\mu_y dt \tag{31}$$

$$d\lambda_t = k_\lambda(\bar{\lambda} - \lambda_t)dt + \sigma_\lambda\sqrt{\lambda_t}dB_t^\lambda \tag{32}$$

where S_t is the price of the asset, α is the expected return, and k_σ and k_λ capture the speed of mean reversion for the variance and the jump intensity who have long-term means of $\bar{\sigma}^2$ and $\bar{\lambda}$. The B_t^σ and B_t^S are Brownian motions with correlation ρ and B_t^λ is a Brownian motion that is independent of the other Brownian motions. N_t is a Poisson counter with intensity λ_t that is independent of the Brownian motions. The average jump size is x, which is normally distributed with mean μ_x and variance σ_x^2. The jump size in variance, y, is exponentially distributed with mean μ_y. Jump sizes are independent of each other and on N_t, and they are independent over time.

Zhen and Zhang (2020) shows that for short horizons, which they find to be less than a year, the following expression is a good approximation of the theoretical skewness:[15]

$$SK_{t,T} = \frac{\lambda_t\mu_{x^3}}{(\sigma_t^2 + \lambda_t\mu_{x^2})^{3/2}\sqrt{T-t}} + \sqrt{T-t}\frac{3\rho\sigma_\sigma\sigma_t^2 + 3\lambda_t\mu_{xy} - \frac{3}{2}\lambda_t\mu_{x^2y}}{2(\sigma_t^2 + \lambda_t\mu_{x^2})^{3/2}} \tag{33}$$

$$+ \mu_{x^3}\frac{3\lambda_t(k_\sigma(\sigma_t^2 - \bar{\sigma}^2) + \rho\sigma_\sigma\sigma_t^2 + \lambda_t\mu_{xy}) + k_\lambda(\lambda_t - \bar{\lambda})(\lambda_t\mu_{x^2} - 2\sigma_t^2)}{4(\sigma_t^2 + \lambda_t\mu_{x^2})^{5/2}} \tag{34}$$

where $\mu_{x^3} = 3\mu_x\sigma_x^2 + \mu_x^3$, $\mu_{x^2y} = (\mu_x^2 + \sigma_x^2)\mu_y$, and $\mu_{xy} = \mu_x\mu_y$.

In Figure 10, we choose parameter values: $\sigma_x = 0.05$, $\mu_x = -0.2$, $\sigma = 0.2$ average annualized volatility of 20%, $T - t = 1/12$, $k_\lambda = 3$, $\bar{\lambda} = 0.0355$ (as in the Wachter (2013) model), $k_\sigma = 2$, $\bar{\sigma}^2 = 0.06$, $\rho = -0.7$, $\sigma_\sigma = 0.6$, $\mu_y = 0.1$.

In the following, we investigate the skewness in several sub-models.

---

[15]Remark 1 of the paper.

D.1 Merton jump diffusion model

In a standard Merton jump diffusion model, the return process takes the form:

$$\frac{dS_t}{S_t} = \alpha dt + \sigma dB_t^S + (e^x - 1)dN_t - \lambda E(e^x - 1)dt \tag{35}$$

This model implies a return skewness over the period from t to T:

$$SK_{t,T}^{Merton} = \frac{\lambda \mu_{x^3}}{(\sigma^2 + \lambda \mu_{x^2})^{3/2}\sqrt{T - t}} \tag{36}$$

where $\mu_{x^3} = 3\mu_x \sigma_x^2 + \mu_x^3 < 0$ and $\mu_{x^2} = \mu_x^2 + \sigma_x^2 > 0$. The first derivative of the skewness wrt. the jump intensity λ is:

$$\frac{dSK_{t,T}^{Merton}}{d\lambda} = \frac{\mu_{x^3}(2\sigma^2 - \lambda \mu_{x^2})}{2\sqrt{T - t}(\lambda \mu_{x^2} + \sigma^2)^{5/2}} \tag{37}$$

Since $\mu_{x^3} < 0$, then $\frac{dSK_{t,T}^{Merton}}{d\lambda} < 0$ if $2\sigma^2 - \lambda \mu_{x^2} > 0$. This is true if jumps are infrequent and if the average jump size and jump variance is not too large. If jumps happen all the time (λ is very large) then the distribution will shift to the left and be "centered" around the jump distribution. In this case, the diffusive part will drive up the skewness of the distribution when the jump intensity increases.

D.2 Adding time varying intensity

The return process is now:

$$\frac{dS_t}{S_t} = \alpha dt + \sqrt{\sigma}dB_t^S + (e^x - 1)dN_t - \lambda_t E(e^x - 1)dt \tag{38}$$

with a mean-reverting jump intensity process:

$$d\lambda_t = k_\lambda(\bar{\lambda} - \lambda_t)dt + \sigma_\lambda \sqrt{\lambda_t}dB_t^\lambda \tag{39}$$

This model implies an approximate return skewness over the period from t to T:

$$SK_{t,T}^{\lambda} = \frac{\lambda_t \mu_{x^3}}{(\sigma^2 + \lambda_t \mu_{x^2})^{3/2}\sqrt{T-t}} \tag{40}$$

$$+ \mu_{x^3}\sqrt{T-t}\frac{k_\lambda(\bar{\lambda} - \lambda_t)[2\sigma^2 - \lambda_t \mu_{x^2}]}{4(\sigma^2 + \lambda_t \mu_{x^2})^{5/2}} \tag{41}$$

D.3   Adding time varying diffusive variance

The return process is now:

$$\frac{dS_t}{S_t} = \alpha dt + \sqrt{\sigma_t}dB_t^S + (e^x - 1)dN_t - \lambda_t E(e^x - 1)dt \tag{42}$$

with a mean-reverting diffusive variance process:

$$d\sigma_t^2 = k_\sigma(m - \sigma_t^2)dt + \sigma_\sigma\sqrt{\sigma_t^2}dB_t^\sigma \tag{43}$$

This model implies an approximate return skewness over the period from t to T:

$$SK_{t,T}^{\lambda,\sigma} = \frac{\lambda_t \mu_{x^3}}{(\sigma_t^2 + \lambda_t \mu_{x^2})^{3/2}\sqrt{T-t}} \tag{44}$$

$$+ \mu_{x^3}\sqrt{T-t}\frac{k_\lambda(\bar{\lambda} - \lambda_t)[2\sigma_t^2 - \lambda_t \mu_{x^2}]}{4(\sigma_t^2 + \lambda_t \mu_{x^2})^{5/2}} \tag{45}$$

$$- \mu_{x^3}\sqrt{T-t}\frac{3\lambda_t k_\sigma(\bar{\sigma}^2 - \sigma_t^2)}{4(\sigma_t^2 + \lambda_t \mu_{x^2})^{5/2}} \tag{46}$$

D.4   Adding correlation between diffusive variance and returns

The return process is now:

$$\frac{dS_t}{S_t} = \alpha dt + \sqrt{\sigma_t}dB_t^S + (e^x - 1)dN_t - \lambda_t E(e^x - 1)dt \tag{47}$$

with a a non-zero correlation between the Brownian motions B_t^S and B_t^σ. This model implies an approximate return skewness over the period from t to T:

$$SK_{t,T}^{\lambda,\sigma,\rho} = \frac{\lambda_t \mu_{x^3}}{(\sigma_t^2 + \lambda_t \mu_{x^2})^{3/2} \sqrt{T-t}} \tag{48}$$

$$+ \mu_{x^3} \sqrt{T-t} \frac{k_\lambda(\bar{\lambda} - \lambda_t)[2\sigma_t^2 - \lambda_t \mu_{x^2}]}{4(\sigma_t^2 + \lambda_t \mu_{x^2})^{5/2}} \tag{49}$$

$$- \mu_{x^3} \sqrt{T-t} \frac{3\lambda_t k_\sigma(\bar{\sigma}^2 - \sigma_t^2)}{4(\sigma_t^2 + \lambda_t \mu_{x^2})^{5/2}} \tag{50}$$

$$+ \sqrt{T-t} \frac{3\rho\sigma_\sigma\sigma_t^2(\lambda_t(2\mu_{x^2} + \mu_{x^3}) + 2\sigma_t^2)}{4(\sigma_t^2 + \lambda_t \mu_{x^2})^{5/2}} \tag{51}$$

D.5 Adding jumps in diffusive variance (contemporaneous with jumps in returns)

The return process is now:

$$\frac{dS_t}{S_t} = \alpha dt + \sqrt{\sigma_t} dB_t^S + (e^x - 1)dN_t - \lambda_t E(e^x - 1)dt \tag{52}$$

with a mean-reverting diffusive variance process with jumps:

$$d\sigma_t^2 = k_\sigma(m - \sigma_t^2)dt + \sigma_\sigma \sqrt{\sigma_t^2} dB_t^\sigma + y dN_t - \lambda_t \mu_y dt \tag{53}$$

This model implies an approximate return skewness over the period from t to T:

$$SK_{t,T}^{\lambda,\sigma,\rho,y} = \frac{\lambda_t \mu_{x^3}}{(\sigma_t^2 + \lambda_t \mu_{x^2})^{3/2} \sqrt{T-t}} \tag{54}$$

$$+ \mu_{x^3} \sqrt{T-t} \frac{k_\lambda(\bar{\lambda} - \lambda_t)[2\sigma_t^2 - \lambda_t \mu_{x^2}]}{4(\sigma_t^2 + \lambda_t \mu_{x^2})^{5/2}} \tag{55}$$

$$- \mu_{x^3} \sqrt{T-t} \frac{3\lambda_t k_\sigma(\bar{\sigma}^2 - \sigma_t^2)}{4(\sigma_t^2 + \lambda_t \mu_{x^2})^{5/2}} \tag{56}$$

$$+ \sqrt{T-t} \frac{3\rho\sigma_\sigma\sigma_t^2(\lambda_t(2\mu_{x^2} + \mu_{x^3}) + 2\sigma_t^2)}{4(\sigma_t^2 + \lambda_t \mu_{x^2})^{5/2}} \tag{57}$$

$$+ \sqrt{T-t} \frac{3\lambda_t(-\lambda_t \mu_{x^2}\mu_{x^2y} + 2\lambda_t \mu_{x^2}\mu_{xy} + \lambda_t \mu_{x^3}\mu_{xy} - \mu_{x^2y}\sigma_t^2 + 2\mu_{xy}\sigma_t^2)}{4(\sigma_t^2 + \lambda_t \mu_{x^2})^{5/2}} \tag{58}$$

Appendix E   Details on Simulation Studies of Disaster Models

E.1   Wachter (2013)

In the Wachter (2013) model, we simulate a time series of 252,000,000 daily jump intensities, stock market returns, treasure bond returns, and dividend/price ratios.[16] This corresponds to 1,000,000 years of data. We then cut the sample into months, where each month is 21 days long (similar to the average number of business days in a month). Within each month, we compute the: (i) expected excess return, (ii) variance, (iii) skewness, and (iv) kurtosis. This gives us four time-series of length 12,000,000 months. We then sort the moments into 50 equal size buckets based on the ex ante (start of each month) jump intensity. Within each bucket, we compute the average expected return, variance, skewness, and kurtosis. Figure 12 shows the moments as function of the ex ante jump intensity. Figure 13 shows the average skewness and kurtosis against the average variance or dividend/price ratio within each jump intensity bucket. Table A1 shows the parameter values used in the simulation. These are the same as in the published version of the Wachter (2013) paper.

Table A1: **Parameter values used in the simulation of the Wachter (2013) model.**

Parameter	Value
Relative risk aversion, γ	3
Rate of time preferences, β	0.012
Average growth in consumption (normal times), μ	0.0252
Volatility of consumption growth (normal times), σ	0.02
Leverage, ϕ	2.6
Average probability of a rare disaster, $\bar{\lambda}$	0.0355
Mean reversion, κ	0.08
Volatility parameter, σ_λ	0.067

E.2   Gabaix (2012)

Within the Gabaix (2012) disaster model, we estimate the markets risk-neutral moments by: (i) simulating option prices, (ii) converting these prices into a risk-neutral density using

---

[16]We thank Jessica Wachter for providing replication code.

Breeden and Litzenberger (1978), (iii) compute moments of the risk-neutral distribution. In our simulation, we let variation in option prices arise from a time varying recovery rate of the market in case of a disaster. Specifically, we let the size of recovery in case of a disaster be uniform on the interval from 0.1 to 0.95, i.e., if a disaster occurs then the value of the stock market drops by 10% to 90%. Table A2 summarizes monthly horizon parameter values used in the simulation.

Table A2: **Parameter values used in the simulation of the Gabaix (2012) model.**

Parameter	Value
Time preference parameter	0.0055
Risk aversion	3
Growth rate of dividends	0.0021
Volatility of dividends	0.032
Probability of disaster	0.0363
Normal time stock volatility	0.04
Stocks recovery rate	Varies from 0.10 to 0.95

Internet Appendix: Not for Publication
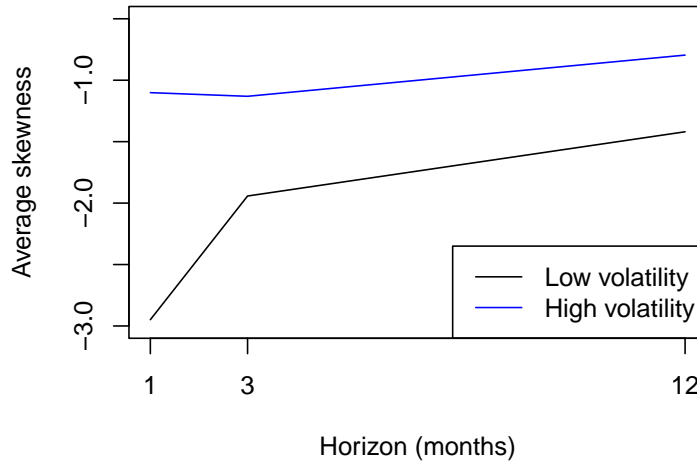
Figure A1: **The term structure of skewness in good and bad times.** This figure shows the average ex ante skewness at different horizons on high/low volatility days. High volatility days are the days in our sample with the 25% highest ex ante variance. Low volatility days are those with the 25% lowest ex ante variances.
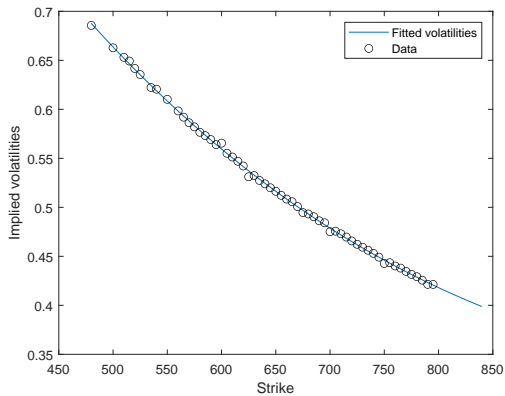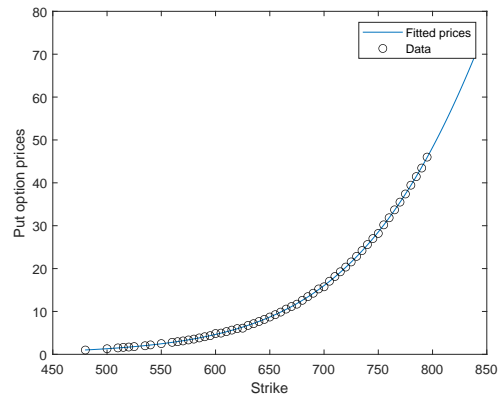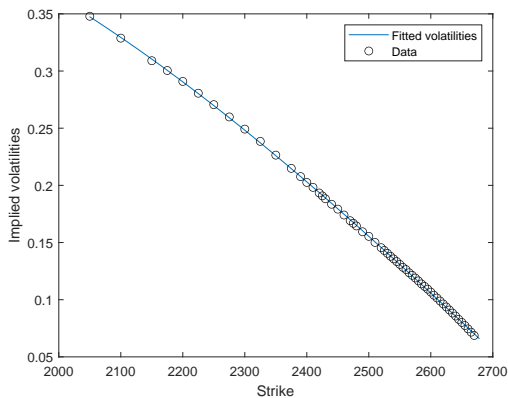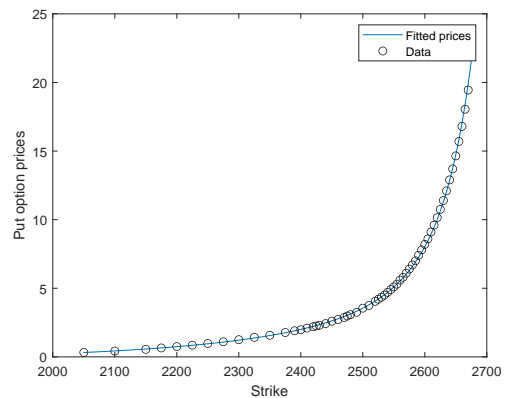
Figure A2: **Examples of fitted implied volatilities.** Subfigures (a) and (b) are from March 31, 2009 using options with a maturity of 46 calendar days. Subfigures (c) and (d) are from Dec. 29, 2017 using options with a maturity of 31 calendar days. The lines in figures (a) and (c) are the fitted implied volatilities from regression (26).
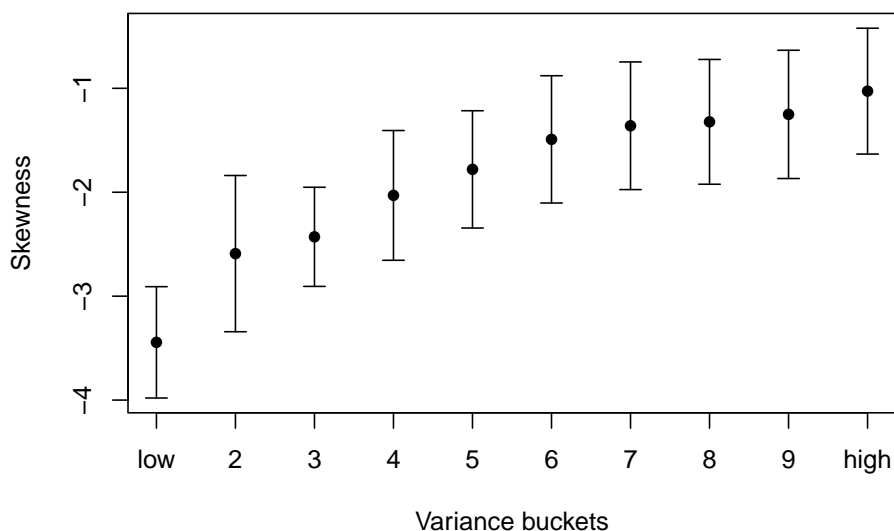
Figure A3: **Skewness in variance buckets.** This figure shows the average ex ante skewness at the monthly horizon for 10 buckets based on the contemporaneous ex ante variance. The low bucket are months with the lowest 10% of ex ante variances, the high bucket is the bucket with the highest 10% of ex ante variance months. The bars represent 95% confidence intervals.

Table A3: **Robustness: Standardized option data versus raw option data.** This table reports the pairwise correlations between the option implied moments while using: (i) all observable option prices and (ii) the volatility surface file from OptionMetrics, which contains option prices with standardized maturities and strikes (in the form of option deltas). For example, the value in 'var' in the SP500 row is the correlation between the option implied variance using (i) and the option implied variance using (ii). The volatility surface contains less observations in the tails of the distributions and therefore the higher-order moments are typically underestimated, which leads to lower correlations for these moments.

	Monthly horizon			Quarterly horizon		
	var	skew	kurt	var	skew	kurt
SP500	0.997	0.794	0.399	0.997	0.908	0.932
NASDAQ	0.993	0.834	0.371	0.987	0.826	0.881
DowJ	0.998	0.751	0.590	0.997	0.951	0.880
Russell	0.995	0.829	0.583	0.987	0.794	0.870

Table A4: **Robustness: Standardized option data.** This table reports the robustness results using standardized option prices from the volatility surface file from OptionMetrics rather than the raw option data. Panel A reports the results when regressing realized moments onto implied moments (as in Table 2). Panel B reports the result when regressing implied higher-order moments onto the implied variance (as in Table 4). Panel C reports the results when regressing implied moments onto the past two-year returns (as in Table 6). Panel D reports the results when regressing implied moments onto the consumption-wealth ratio of Lettau and Ludvigson (2001) (as in Table 8). Variances are annualized and in percentages. We infer expected moments from option prices as discussed in Section 2. The $t-$statistics are corrected for autocorrelation and heteroscedasticity using Newey-West standard errors with 12 lags. We report statistical significance at the 10% level in bold.

| | Monthly horizon | | | | | | Quarterly horizon | | | | | |
| | Skewness | | | Kurtosis | | | Skewness | | | Kurtosis | | |
	β	t-stat.	R^2	β	t-stat.	R^2	β	t-stat.	R^2	β	t-stat.	R^2
Panel A: Implied moments predict realized moments												
SP500	**1.89**	11.18	0.27	**14.76**	10.63	0.39	**2.40**	15.22	0.52	**16.14**	6.55	0.64
NASDAQ	**1.53**	9.12	0.27	**10.73**	10.34	0.28	**1.68**	9.43	0.63	**14.86**	8.35	0.69
DowJ	**1.27**	8.38	0.13	**7.69**	3.96	0.17	**2.00**	10.88	0.47	**14.08**	4.81	0.39
Russell	**1.49**	5.92	0.13	3.82	1.54	0.01	**1.13**	5.41	0.14	**7.96**	4.17	0.05
Panel B: Tail-risk is high when variance is low												
SP500	**0.04**	3.88	0.20	**−0.10**	−3.76	0.25	**0.02**	4.77	0.32	**−0.04**	−4.20	0.35
NASDAQ	**0.03**	11.07	0.54	**−0.03**	−7.21	0.41	**0.01**	10.92	0.64	**−0.01**	−4.52	0.36
DowJ	**0.04**	4.11	0.23	**−0.09**	−3.00	0.16	**0.02**	4.96	0.36	**−0.04**	−4.93	0.39
Russell	**0.03**	4.57	0.20	**−0.04**	−2.89	0.18	**0.01**	4.15	0.23	**−0.02**	−3.27	0.24
Panel C: Cyclicality in higher-moment risk — Past returns												
SP500	**−0.36**	−2.07	0.09	**0.59**	1.66	0.05	−0.30	−1.46	0.06	0.45	1.23	0.03
NASDAQ	0.03	0.24	0.00	−0.10	−0.77	0.02	0.11	0.73	0.02	−0.03	−0.32	0.00
DowJ	**−0.54**	−2.86	0.13	0.55	1.32	0.02	**−0.43**	−1.93	0.09	0.68	1.60	0.05
Russell	**−0.28**	−2.14	0.06	0.20	1.10	0.01	**−0.25**	−1.87	0.05	0.29	1.58	0.03
Panel D: Cyclicality in higher-moment risk — Cay												
SP500	**12.87**	5.78	0.46	**−28.34**	−5.35	0.44	**14.38**	6.54	0.57	**−28.20**	−5.88	0.55
NASDAQ	**13.05**	6.12	0.50	**−16.80**	−6.09	0.47	**17.68**	7.58	0.62	**−16.48**	−9.49	0.64
DowJ	**12.99**	5.08	0.36	**−29.26**	−5.04	0.32	**15.06**	6.02	0.55	**−30.83**	−5.81	0.54
Russell	**6.96**	3.98	0.19	**−13.31**	−3.71	0.27	**10.04**	5.53	0.38	**−15.07**	−5.23	0.47

Table A5: **Robustness: Ex ante moments predict ex post realized moments.** This table replicates the results in main Table 2 while using alternative data choices in the estimation of implied moments as discussed in Appendix A. The first rows of each panel reports the slope coefficients from panel regressions of the form:

$$\text{Realized moment}^i_{t,T} = \alpha^i + \beta E_t[\text{Moment}^i_{t,T}] + \epsilon^i_{t,T}$$

where i represent the different indexes. We include index fixed effects and cluster standard errors by time and country. The second row of each panel reports a similar panel regression, but here we standardize the (standardized) moments within each index before pooling them together and running the regression. We infer the expected moments from option prices and we use methods described in Neuberger (2012) and Bae and Lee (2021) to infer realized moments (see Section 2). We report statistical significance at the 10% level in bold.

| | Month | | | | | | Quarter | | | | | |
| | Skewness | | | Kurtosis | | | Skewness | | | Kurtosis | | |
	β	t-stat.	R^2	β	t-stat.	R^2	β	t-stat.	R^2	β	t-stat.	R^2
Panel A: Detrended moments using all observable prices												
Raw moments	**0.13**	2.24	0.15	0.13	1.61	0.05	**0.27**	3.11	0.31	**0.12**	2.11	0.12
Standardized moments	**0.14**	2.62	0.01	**0.11**	3.46	0.01	**0.26**	5.41	0.05	**0.17**	3.88	0.02
Panel B: Dynamic bounds with extrapolation												
Raw moments	**0.61**	5.42	0.22	**1.96**	6.50	0.09	**0.91**	5.84	0.37	**2.79**	7.22	0.12
Standardized moments	**0.25**	7.76	0.06	**0.25**	7.71	0.06	**0.34**	7.35	0.11	**0.28**	6.95	0.07
Panel C: Static bounds without extrapolation												
Raw moments	**0.29**	3.35	0.17	**0.55**	4.45	0.07	**0.88**	6.76	0.44	0.92	1.47	0.10
Standardized moments	**0.20**	5.09	0.04	**0.20**	4.12	0.04	**0.39**	8.47	0.14	**0.34**	5.40	0.11
Panel D: Static bounds with extrapolation												
Raw moments	**0.49**	4.46	0.22	**0.92**	3.48	0.08	**0.63**	5.20	0.39	**0.93**	2.06	0.10
Standardized moments	**0.24**	5.88	0.06	**0.26**	5.68	0.07	**0.32**	7.61	0.09	**0.26**	4.69	0.06

Table A6: **Robustness: Comovements in higher-moment risks.** This table replicates the results in the first six columns of main Table 3 while using alternative data choices in the estimation of implied moments as discussed in Appendix A. The first rows of each panel reports the slope coefficients from panel regressions of the form:

$$E_t[\text{Skewness}_{t,T}^i] = \alpha^i + \beta E_t[\text{Kurtosis}_{t,T}^i] + \epsilon_{t,T}^i$$

where i represent the different indexes. We include index fixed effects and cluster standard errors by time and country. The second row of each panel reports a similar panel regression, but here we standardize the (standardized) moments within each index before pooling them together and running the regression. We infer the expected moments from option prices (see Section 2). We report statistical significance at the 10% level in bold.

| | Ex ante implied moments | | | | | |
| | Monthly | | | Quarterly | | |
	β	t-stat.	R^2	β	t-stat.	R^2
Panel A: Detrended moments using all observable prices						
Raw moments	**−0.04**	−12.90	0.69	−0.01	−0.21	0.00
Standardized moments	**−0.74**	−8.59	0.54	**−0.67**	−7.34	0.44
Panel B: Dynamic bounds with extrapolation						
Raw moments	**−0.10**	−12.86	0.64	**−0.10**	−9.17	0.73
Standardized moments	**−0.76**	−24.15	0.58	**−0.80**	−18.10	0.64
Panel C: Static bounds without extrapolation						
Raw moments	**−0.07**	−16.21	0.83	−0.01	−0.21	0.33
Standardized moments	**−0.84**	−22.25	0.71	**−0.74**	−6.54	0.54
Panel D: Static bounds with extrapolation						
Raw moments	**−0.07**	−8.00	0.69	−0.02	−0.36	0.32
Standardized moments	**−0.77**	−22.48	0.59	**−0.70**	−6.37	0.49

Table A7: **Robustness: Tail-risk is high when variance is low — Ex ante implied moments.** This table replicates the results in main Table 4 while using alternative data choices in the estimation of implied moments as discussed in Appendix A. The first rows of each panel reports the slope coefficients from panel regressions of the form:

$$E_t[\text{Moment}_{t,T}^i] = \alpha^i + \beta E_t[\text{Variance}_{t,T}^i] + \epsilon_{t,T}^i$$

where i represent the different indexes. We include index fixed effects and cluster standard errors by time and country. The second row of each panel reports a similar panel regression, but here we standardize the (standardized) moments within each index before pooling them together and running the regression. We infer the expected moments from option prices (see Section 2). We report statistical significance at the 10% level in bold.

	Month						Quarter					
	Skewness			Kurtosis			Skewness			Kurtosis		
	β	t-stat.	R^2	β	t-stat.	R^2	β	t-stat.	R^2	β	t-stat.	R^2
Panel A: Detrended moments using all observable prices												
Raw moments	**0.07**	7.63	0.08	**−1.02**	−5.30	0.05	**0.03**	3.42	0.02	**−0.45**	−2.55	0.01
Standardized moments	**0.33**	6.17	0.11	**−0.24**	−8.33	0.05	**0.29**	4.82	0.08	**−0.24**	−5.76	0.05
Panel B: Dynamic bounds with extrapolation												
Raw moments	**0.01**	2.29	0.27	**−0.14**	−4.26	0.34	**0.02**	2.07	0.37	**−0.18**	−3.54	0.39
Standardized moments	**0.15**	3.95	0.02	**−0.28**	−6.38	0.08	**0.24**	3.72	0.07	**−0.32**	−5.61	0.09
Panel C: Static bounds without extrapolation												
Raw moments	**0.06**	5.27	0.32	**−0.84**	−5.22	0.29	**0.05**	4.32	0.43	**−0.39**	−3.89	0.30
Standardized moments	**0.35**	7.62	0.12	**−0.40**	−7.34	0.16	**0.45**	7.31	0.20	**−0.55**	−9.01	0.30
Panel D: Static bounds with extrapolation												
Raw moments	**0.04**	3.95	0.35	**−0.44**	−3.82	0.29	**0.03**	3.66	0.36	**−0.41**	−3.79	0.32
Standardized moments	**0.36**	5.54	0.13	**−0.45**	−5.97	0.20	**0.34**	5.48	0.11	**−0.47**	−8.05	0.21

Table A8: **Non-linear relation between moments.** The table reports the slope coefficients from regressions of the form:

$$E_t[\text{Moment}_{t,T}] = \alpha + \begin{bmatrix} \beta_1 \\ \beta_2 \\ \beta_2 \end{bmatrix}^T \begin{bmatrix} E_t[\text{Variance}_{t,T}] \\ E_t[\text{Variance}_{t,T}]^2 \\ E_t[\text{Variance}_{t,T}]^3 \end{bmatrix} + \epsilon_{t,T}$$

where $E_t[\text{Moment}_{t,T}]$ is either the ex ante skewness or the ex ante kurtosis of the S&P 500 index. We infer the expected moments from option prices, The $t-$statistics are corrected for autocorrelation and heteroscedasticity using Newey-West standard errors with 12 lags. We report statistical significance at the 10% level in bold.

	Month						Quarter					
	Skewness			Kurtosis			Skewness			Kurtosis		
β_1	**0.13**	**0.36**	**0.73**	**−2.14**	**−6.43**	**−12.92**	**0.12**	**0.35**	**0.69**	**−0.72**	**−2.50**	**−5.17**
	(3.82)	(5.18)	(5.79)	(−3.29)	(−4.77)	(−5.44)	(4.83)	(3.50)	(2.97)	(−3.84)	(−3.85)	(−3.18)
β_2		**−0.01**	**−0.06**		**0.21**	**0.99**		**−0.02**	**−0.07**		**0.12**	**0.56**
		(−3.84)	(−4.71)		(3.80)	(4.63)		(−2.65)	(−2.36)		(3.42)	(2.73)
β_3			**0.00**			**−0.02**			**0.00**			**−0.02**
			(4.19)			(−4.18)			(2.04)			(−2.49)
R^2	0.22	0.36	0.44	0.14	0.25	0.30	0.31	0.40	0.43	0.31	0.47	0.51

Table A9: **Robustness: Cyclicality in higher-moment risks — Ex ante implied moments.** This table replicates the results in main Table 6 while using alternative data choices in the estimation of implied moments as discussed in Appendix A. The first rows of each panel reports the slope coefficients from panel regressions of the form:

$$E_t[\text{Moment}^i_{t,T}] = \alpha^i + \beta r^i_{t-24,t} + \epsilon^i_{t,T}$$

where i represent the different indexes and $r^i_{t-24,t}$ is the return on index i from $t-24$ to t. We include index fixed effects and cluster standard errors by time and country. The second row of each panel reports a similar panel regression, but here we standardize the (standardized) moments within each index before pooling them together and running the regression. We infer the expected moments from option prices (see Section 2). We report statistical significance at the 10% level in bold.

	Month						Quarter					
	Skewness			Kurtosis			Skewness			Kurtosis		
	β	t-stat.	R^2	β	t-stat.	R^2	β	t-stat.	R^2	β	t-stat.	R^2
Panel A: Detrended moments using all observable prices												
Raw moments	**−0.85**	−4.31	0.04	**9.01**	2.17	0.01	**−0.49**	−3.65	0.01	**5.98**	2.50	0.01
Standardized moments	**−0.24**	−6.17	0.05	**0.11**	3.09	0.01	**−0.27**	−5.18	0.06	**0.21**	5.27	0.03
Panel B: Dynamic bounds with extrapolation												
Raw moments	−0.14	−1.79	0.26	**1.29**	1.91	0.31	−0.18	−1.39	0.37	**2.31**	2.18	0.37
Standardized moments	**−0.09**	−2.28	0.01	**0.11**	2.14	0.01	**−0.13**	−1.91	0.01	**0.19**	2.84	0.03
Panel C: Static bounds without extrapolation												
Raw moments	**−0.65**	−3.22	0.27	**8.15**	2.98	0.22	**−0.42**	−2.99	0.36	**3.04**	2.54	0.21
Standardized moments	**−0.21**	−3.85	0.04	**0.20**	3.34	0.03	**−0.27**	−3.80	0.07	**0.29**	3.66	0.08
Panel D: Static bounds with extrapolation												
Raw moments	**−0.45**	−3.09	0.30	**4.42**	2.78	0.21	**−0.26**	−1.84	0.32	**3.77**	2.44	0.24
Standardized moments	**−0.23**	−4.25	0.05	**0.22**	3.57	0.05	**−0.17**	−2.33	0.02	**0.25**	3.42	0.05

Table A10: **Cyclicality in higher-moment risks — Book-to-Market (Ex ante implied moments).** The first row of Panel A reports the slope coefficients from panel regressions of the form:

$$E_t[\text{Moment}^i_{t,T}] = \alpha^i + \beta \text{Book-to-market}^i_t + \gamma t + \epsilon^i_{t,T}$$

where i represent the different indexes and Book-to-market^i_t is the book-to-market ratio of index i at time$t$. We include index fixed effects and cluster standard errors by time and country. The second row of Panel A reports a similar panel regression, but here we standardize the (standardized) moments and the past returns within each index before pooling them together and running the regression. Panel B reports univariate regressions of expected moments onto the past returns for each individual index. We infer the expected moments from option prices (see Section 2). The $t-$statistics in the individual index-wise regressions are corrected for autocorrelation and heteroscedasticity using Newey-West standard errors with 12 lags. We report statistical significance at the 10% level in bold.

| | Monthly horizon | | | | | | Quarterly horizon | | | | | |
| | Skewness | | | Kurtosis | | | Skewness | | | Kurtosis | | |
	β	t-stat.	R^2	β	t-stat.	R^2	β	t-stat.	R^2	β	t-stat.	R^2
Panel A: Pooled panel regressions												
Raw moments	**1.29**	2.52	0.02	**−13.59**	−2.02	0.00	0.16	0.4	−0.01.	−5.70	−1.20	−0.00
Standardized moments	**0.18**	4.36	0.03	−0.06	−1.10	−0.00	**0.13**	1.86	0.00	−0.09	−1.63	−0.00
Panel B: Index-wise regressions												
United States												
SP500	**3.00**	3.18	0.29	−23.88	−1.38	0.02	**2.19**	2.05	0.44	**−9.84**	−2.02	0.38
NASDAQ	0.30	0.36	0.29	**22.07**	2.35	0.06	0.88	1.43	0.37	0.80	0.28	0.45
DowJ	**3.14**	1.84	0.21	−1.85	−0.06	0.10	1.26	1.14	0.35	−3.99	−0.54	0.19
Russell	**2.11**	2.52	0.19	7.73	1.20	0.13	**2.49**	3.60	0.22	−2.23	−0.69	0.35
Europe												
BEL	−0.14	−0.62	0.02	−3.83	−1.25	0.00	−0.18	−0.70	−0.02	1.19	1.54	−0.01
CHE	**5.75**	3.98	0.11	**−115.74**	−3.11	0.05	**1.76**	2.74	0.55	**−20.17**	−3.04	0.41
DEU	**2.99**	3.52	0.10	**−61.97**	−3.40	0.07	**1.30**	2.32	0.30	**−23.53**	−3.19	0.12
ESP	**1.42**	2.12	0.03	**−15.53**	−2.77	0.12	**0.99**	3.37	0.17	**−4.84**	−3.49	0.06
FIN	**0.95**	4.77	0.07	**−1.97**	−1.77	−0.03	**1.94**	4.00	0.13	**−2.65**	−2.95	0.13
FRA	**1.89**	4.67	0.22	**−26.46**	−3.23	0.11	**1.39**	2.97	0.23	**−9.50**	−2.10	0.11
GBR	**5.54**	4.41	0.38	**−91.74**	−3.17	0.36	**2.17**	2.33	0.21	**−28.07**	−1.82	0.18
ITA	**3.25**	3.74	0.13	**−40.47**	−3.50	0.11	**2.46**	2.92	0.25	**−31.12**	−2.13	0.20
NLD	0.91	1.24	0.10	−9.97	−0.55	0.03	−1.89	−1.55	0.13	−29.84	−1.65	−0.01
SWE	2.08	1.65	0.08	−31.33	−1.52	0.05	**1.59**	2.65	0.11	**−18.25**	−2.21	0.05
Asia												
AUS	−1.36	−0.51	0.01	58.56	1.00	0.01	−3.01	−1.36	0.06	50.32	1.29	0.02
HKG	−0.06	−0.10	0.03	2.83	0.38	0.02	0.06	0.14	0.01	−0.97	−0.39	0.08
JPN	−0.44	−0.72	0.64	7.25	0.60	0.54	**−1.54**	−2.34	0.65	7.08	0.88	0.46

Table A11: **Cyclicality in higher-moment risks — Book-to-Market (Ex post realized moments).** The first row of Panel A reports the slope coefficients from panel regressions of the form:

$$\text{Realized moment}^i_{t,T} = \alpha^i + \beta \text{Book-to-market}^i_t + \gamma t + \epsilon^i_{t,T}$$

where i represent the different indexes and Book-to-market^i_t is the book-to-market ratio of index i at time$t$. We include index fixed effects and cluster standard errors by time and country. The second row of Panel A reports a similar panel regression, but here we standardize the (standardized) moments and the past returns within each index before pooling them together and running the regression. Panel B reports univariate regressions of expected moments onto the past returns for each individual index. We infer the expected moments from option prices (see Section 2). The $t-$statistics in the individual index-wise regressions are corrected for autocorrelation and heteroscedasticity using Newey-West standard errors with 12 lags. We report statistical significance at the 10% level in bold.

| | Monthly horizon | | | | | | Quarterly horizon | | | | | |
| | Skewness | | | Kurtosis | | | Skewness | | | Kurtosis | | |
	β	t-stat.	R^2	β	t-stat.	R^2	β	t-stat.	R^2	β	t-stat.	R^2
Panel A: Pooled panel regressions												
Raw moments	0.40	0.89	0.13	−4.80	−0.55	0.04	0.28	0.43	0.26	−20.40	−1.61	0.10
Standardized moments	0.05	1.39	−0.00	**−0.05**	−1.73	−0.00	0.06	0.90	−0.01	**−0.12**	−2.54	0.00
Panel B: Index-wise regressions												
United States												
SP500	**1.56**	2.20	0.11	**−45.67**	−3.61	0.15	0.93	0.83	0.31	**−31.05**	−2.33	0.31
NASDAQ	−0.33	−0.57	0.19	−4.24	−0.95	0.20	−0.59	−0.78	0.45	−2.14	−0.34	0.47
DowJ	0.41	0.53	0.02	−11.39	−1.25	0.03	0.09	0.09	0.19	−16.80	−1.04	0.18
Russell	0.59	0.76	0.00	**−16.78**	−1.71	0.04	0.88	0.99	0.00	−9.50	−0.75	−0.01
Europe												
BEL	**−0.70**	−1.75	0.12	**20.50**	3.17	0.06	−0.92	−1.54	0.16	5.80	0.59	0.01
CHE	−0.11	−0.11	0.08	7.42	0.24	0.00	**2.91**	2.56	0.23	**−103.13**	−3.54	0.13
DEU	**2.07**	2.09	0.05	−8.79	−0.36	0.02	2.15	1.01	0.17	−63.16	−0.91	0.13
ESP	**1.04**	2.22	0.02	−21.01	−1.42	−0.01	**2.12**	3.52	0.12	**−40.69**	−3.24	0.08
FIN	0.03	0.04	−0.03	−9.41	−0.67	−0.03	**3.18**	3.34	0.08	−30.15	−1.19	0.02
FRA	**1.93**	2.50	0.01	−25.23	−1.43	0.00	**2.89**	2.26	0.09	−65.31	−1.59	0.08
GBR	0.11	0.11	−0.01	−4.35	−0.18	−0.01	−0.34	−0.26	0.11	**−71.64**	−2.74	0.07
ITA	0.60	1.32	0.00	−4.56	−0.25	−0.01	**2.21**	3.04	0.20	**−62.21**	−3.58	0.08
NLD	**1.27**	1.79	0.00	−17.73	−1.01	−0.01	0.44	0.46	0.11	−30.91	−1.59	0.03
SWE	**1.98**	1.76	0.08	−32.52	−1.33	0.02	**3.96**	2.20	0.37	**−66.71**	−1.92	0.13
Asia												
AUS	1.12	1.20	0.01	−25.05	−0.58	−0.01	**−3.86**	−2.24	0.04	−20.62	−0.59	−0.03
HKG	−1.28	−0.52	0.00	11.99	0.50	0.00	−1.82	−0.93	0.01	12.26	0.71	0.00
JPN	0.17	0.10	0.05	5.74	0.24	0.11	**−3.37**	−2.05	0.18	**48.34**	1.74	0.25

Table A12: **Cyclicality in higher-moment risks — Past two-year return (Ex ante implied moments).** The first row of Panel A reports the slope coefficients from panel regressions of the form:

$$E_t[\text{Moment}_{t,T}^i] = \alpha^i + \beta r_{t-24,t}^i + \epsilon_{t,T}^i$$

where i represent the different indexes and $r_{t-24,t}^i$ is the return on index i from $t-24$ to t. We include index fixed effects and cluster standard errors by time and country. The second row of Panel A reports a similar panel regression, but here we standardize the (standardized) moments and the past returns within each index before pooling them together and running the regression. Panel B reports univariate regressions of expected moments onto the past returns for each individual index. We infer the expected moments from option prices (see Section 2). The $t-$statistics in the individual index-wise regressions are corrected for autocorrelation and heteroscedasticity using Newey-West standard errors with 12 lags. We report statistical significance at the 10% level in bold.

	Monthly horizon						Quarterly horizon					
	Skewness			Kurtosis			Skewness			Kurtosis		
	β	t-stat.	R^2	β	t-stat.	R^2	β	t-stat.	R^2	β	t-stat.	R^2
Panel A: Pooled panel regressions												
Raw moments	**−0.84**	−3.39	0.26	**9.74**	2.00	0.17	**−0.53**	−2.87	0.24	**6.01**	2.07	0.17
Standardized moments	**−0.21**	−4.97	0.04	**0.10**	2.18	0.01	**−0.23**	−3.85	0.04	**0.15**	2.61	0.01
Panel B: Index-wise regressions												
United States												
SP500	**−1.30**	−2.91	0.12	8.01	1.28	0.01	**−0.84**	−1.88	0.11	2.79	0.97	0.03
NASDAQ	−0.24	−0.78	0.03	**−4.45**	−3.44	0.08	−0.26	−1.26	0.06	−0.75	−1.13	0.03
DowJ	**−2.29**	−2.99	0.13	9.01	0.56	0.00	**−1.29**	−2.02	0.17	4.66	1.08	0.04
Russell	**−1.04**	−3.46	0.13	1.97	0.39	0.00	**−0.97**	−3.64	0.16	0.75	0.70	0.00
Europe												
BEL	−0.70	−1.30	0.03	13.60	1.58	0.03	−0.63	−1.56	0.09	**3.13**	2.13	0.07
CHE	**−2.64**	−4.17	0.10	**52.23**	3.16	0.07	**−0.89**	−1.73	0.11	**11.33**	2.03	0.11
DEU	**−1.57**	−6.17	0.14	**26.79**	5.44	0.09	**−0.92**	−2.88	0.24	**15.78**	3.79	0.22
ESP	−0.10	−0.15	0.00	0.09	0.01	0.00	−0.42	−1.24	0.05	**3.45**	2.32	0.05
FIN	−0.19	−0.59	0.00	−0.93	−0.49	0.00	**−0.60**	−1.98	0.08	0.85	1.13	0.03
FRA	**−1.23**	−5.31	0.14	**16.27**	4.92	0.08	**−0.92**	−2.87	0.16	**11.32**	2.43	0.17
GBR	**−3.16**	−2.85	0.08	**44.72**	1.71	0.03	**−2.47**	−2.49	0.12	**34.65**	1.97	0.07
ITA	**−1.55**	−3.45	0.07	**19.61**	3.78	0.06	**−1.87**	−3.55	0.12	**24.90**	3.22	0.08
NLD	**−2.20**	−5.39	0.13	**38.75**	3.83	0.07	−0.36	−0.37	−0.01	**35.10**	2.27	0.04
SWE	−0.91	−0.78	0.00	10.59	0.54	0.00	−0.55	−1.23	−0.01	4.35	0.96	−0.01
Asia												
AUS	−0.60	−0.57	0.00	23.28	0.90	0.01	0.07	0.07	−0.01	−2.63	−0.21	−0.01
CHN	0.16	1.47	0.02	**−3.46**	−2.96	0.05	0.02	0.23	−0.01	−1.22	−1.28	0.00
HKG	0.18	0.86	0.00	−3.11	−0.69	0.00	0.12	0.79	0.00	−0.72	−0.61	0.00
JPN	−0.28	−0.31	0.00	2.56	0.18	0.00	0.13	0.13	−0.01	4.03	0.40	0.00
KOR	0.25	0.63	0.00	**−8.99**	−1.85	0.02	0.07	0.29	−0.01	−2.55	−1.40	0.02
TWN	0.05	0.11	0.00	1.82	0.47	0.00	−0.16	−0.41	−0.01	0.54	0.35	−0.01

Table A13: **Cyclicality in higher-moment risks — Past two-year return (Ex post realized moments).** The first row of Panel A reports the slope coefficients from panel regressions of the form:

$$\text{Realized moment}_{t,T}^{i} = \alpha^{i} + \beta r_{t-24,t}^{i} + \epsilon_{t,T}^{i}$$

where i represent the different indexes and $r_{t-24,t}^{i}$ is the return on index i from $t-24$ to t. We include index fixed effects and cluster standard errors by time and country. The second row of Panel A reports a similar panel regression, but here we standardize the (standardized) moments and the past returns within each index before pooling them together and running the regression. Panel B reports univariate regressions of realized moments onto the past returns for each individual index. We use methods described in Neuberger (2012) and Bae and Lee (2021) to infer realized moments (see Section 2). The $t-$statistics in the individual index-wise regressions are corrected for autocorrelation and heteroscedasticity using Newey-West standard errors with 12 lags. We report statistical significance at the 10% level in bold.

| | Monthly horizon | | | | | | Quarterly horizon | | | | | |
| | Skewness | | | Kurtosis | | | Skewness | | | Kurtosis | | |
	β	t-stat.	R^2	β	t-stat.	R^2	β	t-stat.	R^2	β	t-stat.	R^2
Panel A: Pooled panel regressions												
Raw moments	−0.34	−1.63	0.13	**6.35**	1.70	0.04	−0.21	−0.77	0.30	**9.82**	1.86	0.12
Standardized moments	**−0.08**	−2.19	0.00	**0.07**	2.52	0.00	−0.07	−1.06	0.00	**0.10**	2.07	0.00
Panel B: Index-wise regressions												
United States												
SP500	−0.59	−1.59	0.02	**14.94**	3.63	0.05	−0.70	−1.15	0.02	**10.43**	1.91	0.04
NASDAQ	0.07	0.49	0.00	0.16	0.11	0.00	−0.08	−0.33	−0.01	−0.64	−0.35	−0.01
DowJ	**−0.70**	−1.73	0.01	**12.73**	3.29	0.03	−0.85	−1.27	0.03	10.55	1.37	0.01
Russell	**−0.58**	−1.75	0.01	**13.88**	1.67	0.03	**−1.06**	−2.12	0.08	12.68	1.59	0.06
Europe												
BEL	−0.25	−0.51	0.00	4.75	0.42	0.00	−0.89	−1.23	0.03	21.33	1.44	0.03
CHE	−0.25	−0.39	0.00	7.83	0.34	0.00	−1.16	−1.57	0.06	**38.66**	2.64	0.10
DEU	−0.56	−0.98	0.01	8.55	0.43	0.00	−0.20	−0.34	−0.01	0.81	0.07	−0.01
ESP	**−1.41**	−2.51	0.03	**19.08**	1.80	0.00	−0.12	−0.26	−0.01	6.52	0.88	0.00
FIN	−0.14	−0.32	−0.01	19.35	1.35	0.13	−1.25	−1.35	0.06	31.56	1.45	0.04
FRA	**−1.33**	−2.33	0.03	23.33	1.64	0.02	−0.65	−0.85	0.01	12.80	0.85	0.01
GBR	−0.91	−1.47	0.01	**35.66**	1.90	0.01	−0.40	−0.42	0.00	**37.86**	2.33	0.03
ITA	−0.23	−0.49	0.00	−4.41	−0.38	0.00	−0.88	−1.12	0.04	**39.24**	2.12	0.09
NLD	**−2.00**	−2.72	0.06	23.88	1.47	0.00	**−1.95**	−2.99	0.13	**37.55**	2.38	0.09
SWE	**−0.91**	−2.13	0.01	15.38	0.87	0.00	−0.88	−1.20	0.02	**16.85**	1.76	0.01
Asia												
AUS	**−1.94**	−2.66	0.04	**46.02**	2.29	0.03	**1.81**	2.39	0.06	48.39	1.61	0.02
CHN	−0.30	−0.85	0.00	−2.15	−0.44	0.00	0.23	0.80	0.00	−5.27	−1.27	0.01
HKG	0.26	0.35	0.00	−6.18	−0.82	0.00	0.92	1.26	0.03	−8.11	−0.97	0.01
JPN	**1.49**	2.41	0.04	−23.92	−1.51	0.01	**2.50**	2.36	0.16	−26.80	−1.39	0.05
KOR	0.13	0.37	0.00	−4.52	−1.17	0.00	0.62	1.50	0.01	−6.77	−1.40	0.01
TWN	0.36	0.51	0.00	5.69	0.54	0.00	−0.25	−0.29	−0.01	−0.72	−0.10	−0.01

Table A14: **Ex ante higher-order moments and jump tail probabilities.** This table reports the slope coefficients from index-wise regressions on the form:

$$\text{Probability of } -x\sigma_{t,T}^{\text{Black-Scholes ATM}} \text{ event}_{t,T} = \alpha + \beta \text{Moment}_{t,T^*} + \epsilon_{t,T}$$

where $x = 7$ or 10 and $\sigma_{t,T}^{\text{Black-Scholes ATM}}$ is the at-the-money implied Black-Scholes volatility. The Probability of $-x\sigma_{t,T}^{Black-Scholes ATM}$ event$_{t,T}$ is estimated using the methods in Bollerslev, Todorov, and Xu (2015). We infer the expected moments from option prices and we use methods described in Neuberger (2012) and Bae and Lee (2021) to infer realized moments (see Section 2). The asterisk in Moment$_{t,T^*}$ indicates that the maturity of the moments differ from those of the probabilities as discussed in Section 4.2. The $t-$statistics are corrected for autocorrelation and heteroscedasticity using Newey-West standard errors with 12 lags. We report statistical significance at the 10% level in bold.

| | Implied moments | | | | | | Realized moments | | | | | |
| | $x=10$ | | | $x=7$ | | | $x=10$ | | | $x=7$ | | |
	β	t-stat.	R^2	β	t-stat.	R^2	β	t-stat.	R^2	β	t-stat.	R^2
Panel A: ex ante variance												
SP500	**−4.09**	−1.89	0.06	−0.18	−0.08	0.00	**−1.94**	−2.45	0.03	−1.14	−1.25	0.00
NASDAQ	**−2.85**	−1.92	0.11	−2.46	−0.88	0.02	**−1.68**	−1.78	0.06	−1.43	−0.89	0.01
DowJ	**−4.18**	−2.73	0.09	2.49	1.63	0.01	**−2.49**	−3.90	0.06	0.49	0.53	−0.01
Russell	**−2.24**	−1.85	0.07	−1.03	−0.90	0.00	**−1.09**	−2.18	0.04	−0.71	−1.30	0.00
Panel B: ex ante skewness												
SP500	**−0.03**	−5.21	0.42	**−0.03**	−3.98	0.16	**−0.02**	−5.55	0.16	**−0.03**	−7.08	0.16
NASDAQ	**−0.03**	−8.55	0.36	**−0.05**	−6.97	0.20	**−0.02**	−5.31	0.18	**−0.03**	−4.90	0.17
DowJ	**−0.02**	−5.68	0.41	**−0.01**	−2.00	0.05	−0.00	−0.64	0.00	−0.00	−0.82	0.00
Russell	**−0.03**	−3.16	0.30	**−0.04**	−3.27	0.18	−0.01	−1.43	0.02	−0.01	−1.59	0.03
Panel C: ex ante kurtosis												
SP500	**0.06**	1.73	0.07	0.01	0.22	0.00	**0.13**	4.56	0.20	**0.16**	5.88	0.14
NASDAQ	−0.03	−0.58	0.00	−0.10	−0.95	0.01	**0.15**	2.90	0.14	**0.29**	4.08	0.13
DowJ	**0.06**	4.22	0.26	0.03	1.53	0.02	**0.10**	2.73	0.08	0.05	1.40	0.01
Russell	0.12	1.44	0.07	0.11	1.34	0.03	**0.23**	1.90	0.09	0.24	1.55	0.05

Table A15: **Cyclicality in conditional tail probabilities in jump diffusion models.** This table reports the results of regressions on the form:

$$\text{Probability of } -x\sigma_{t,T}^{\text{Black-Scholes ATM}} \text{ event}_{t,T} = \alpha + \beta \text{Indicator}_t + \gamma t + \epsilon_{t,T}$$

where $x = 7$ or 10 and $\sigma_{t,T}^{\text{Black Scholes ATM}}$ is the at-the-money implied Black-Scholes volatility. Indicator$_t$ is either the past 2-year return (Panel A), the consumption-wealth ratio Lettau and Ludvigson (2001) scaled by 100 for readability (Panel B), the dividend-price ratio (Panel C), the book-to-market ratio (Panel D), or NBER recession periods (Panel E). In regressions for the dividend-price ratio and the book-to-market ratio, we add a time trend to the regression. The Probability of $-x\sigma_{t,T}^{Black-ScholesATM}$ event$_{t,T}$ is estimated using the methods in Bollerslev, Todorov, and Xu (2015).The $t-$statistics are corrected for autocorrelation and heteroscedasticity using Newey-West standard errors with 12 lags. We report statistical significance at the 10% level in bold.

	$x = 10$			$x = 7$		
	β	t-stat.	R^2	β	t-stat.	R^2
Panel A: past 2-year return						
SP500	0.03	1.28	0.03	0.04	1.60	0.03
NASDAQ	**0.05**	3.35	0.18	**0.07**	2.71	0.12
DowJ	**0.07**	3.14	0.13	0.01	0.47	0.00
Russell	0.02	1.02	0.02	0.03	0.94	0.01
Panel B: cay						
SP500	**−1.89**	−5.65	0.41	**−1.84**	−5.05	0.18
NASDAQ	**−1.34**	−3.37	0.28	**−2.21**	−3.69	0.20
DowJ	**−1.25**	−1.75	0.13	0.12	0.16	−0.01
Russell	**−1.93**	−3.69	0.39	**−1.65**	−2.58	0.14
Panel C: Dividend-Price Ratio						
SP500	**−2.18**	−2.69	0.40	−0.77	−0.54	0.19
NASDAQ	**1.42**	2.24	0.41	**3.77**	2.57	0.36
DowJ	**−2.97**	−3.71	0.08	**−2.93**	−1.95	0.03
Russell	**−1.65**	−1.68	0.07	−2.61	−1.27	0.01
Panel D: Book-to-Market Ratio						
SP500	**−0.13**	−2.96	0.43	−0.08	−1.40	0.20
NASDAQ	0.04	1.17	0.40	**0.14**	2.13	0.36
DowJ	**−0.11**	−2.97	0.08	**−0.14**	−1.93	0.04
Russell	**−0.15**	−2.76	0.17	**−0.22**	−2.42	0.06
Panel E: NBER recessions						
SP500	−0.03	−1.38	0.03	−0.03	−1.12	0.02
NASDAQ	−0.01	−0.99	0.01	−0.01	−0.38	−0.00
DowJ	**−0.04**	−2.51	0.13	−0.03	−1.10	0.01
Russell	**−0.02**	−1.66	0.03	−0.03	−1.17	0.01